prg
Pierini Research Group

IPPT PAN

Electrospinning of conjugated polymer nanofibers: research challenges and applications

Filippo Pierini

Department of Biosystems and Soft Matter

Institute of Fundamental Technological Research, Polish Academy of Sciences

Outline

- Introduction
  - Conjugated polymers
  - Electrospinning
- Electrospun Polyaniline-Based Composite Nanofibers
  - Technical challenges
  - Tuning the electrical conductivity by tailoring the nanofiller structure
- Electrospun Nanofibers for Organic Photovoltaics
  - The solar cell performance race
  - Single-material organic solar cells based on electrospun fullerene-grafted polythiophene nanofibers
- Summary and future work

A new material class

The Nobel Prize in Chemistry 2000

"for the discovery and development of conductive polymers"

Alan J. Heeger	Alan G. MacDiarmid	Hideki Shirakawa
1/3 of the prize	1/3 of the prize	1/3 of the prize
USA	USA and New Zealand	Japan
University of California Santa Barbara, CA, USA	University of Pennsylvania Philadelphia, PA, USA	University of Tsukuba Tokyo, Japan
b. 1936	b. 1927 (in Masterton, New Zealand)	b. 1936

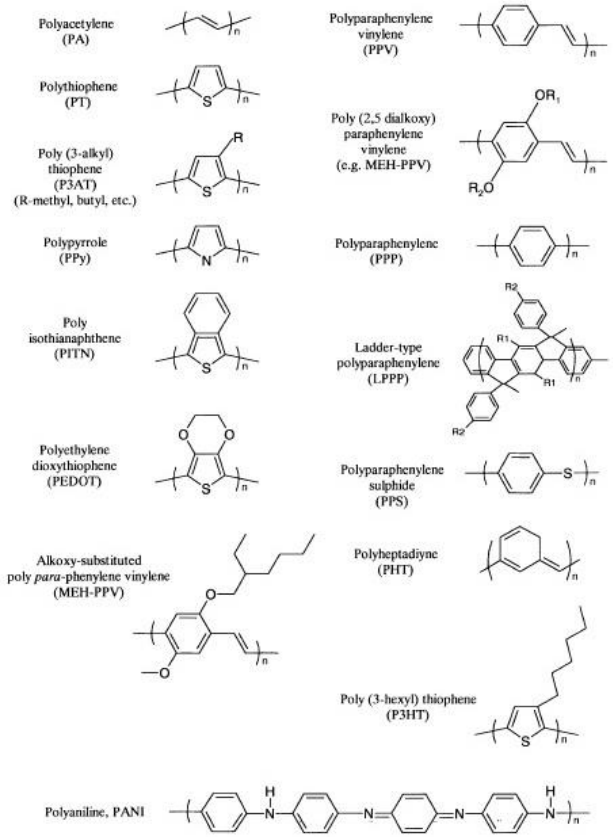

“Synthetic metals” which combine chemical and mechanical properties of polymers with electronic properties of metals and novel optical properties.

Inexpensive to make, flexible, light-weight, and stable.

Polymers with Unsaturated (Conjugated) backbone structure

A conjugated main chain with alternating single and double bond.

First example of conjugate polymer:

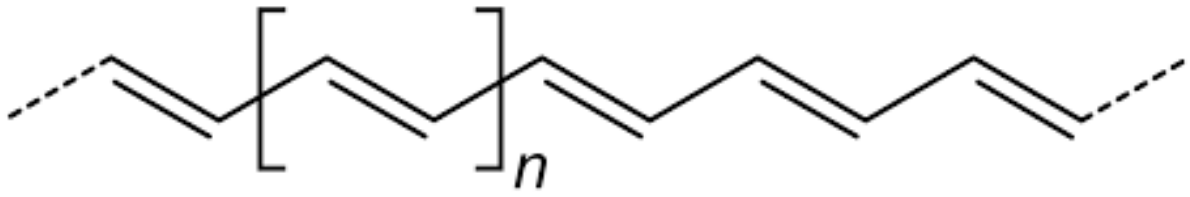

Polyacetylene

Synthesized (by serendipity) - Shirakawa

Conductive polymers

1- The first condition for this is that the polymer consists of alternating single and double bonds, called conjugated double bonds.

2- The second condition is that the plastic has to be disturbed because full orbital can not conduct electrons, so to get a conjugated material to conduct:

- removing electrons from the HOMO creating holes (oxidation)
- inserting electrons to LUMO (reduction)

⇒ DOPING

15-puzzle

The game offers a simple model of a doped polymer. The pieces cannot move unless there is at least one empty "hole".
In the polymer each piece is an electron that jumps to a hole vacated by another one. This creates a movement along the molecule - an electric current.

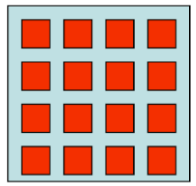

It can not move pieces

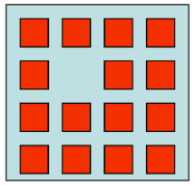

It can move pieces

Doping process

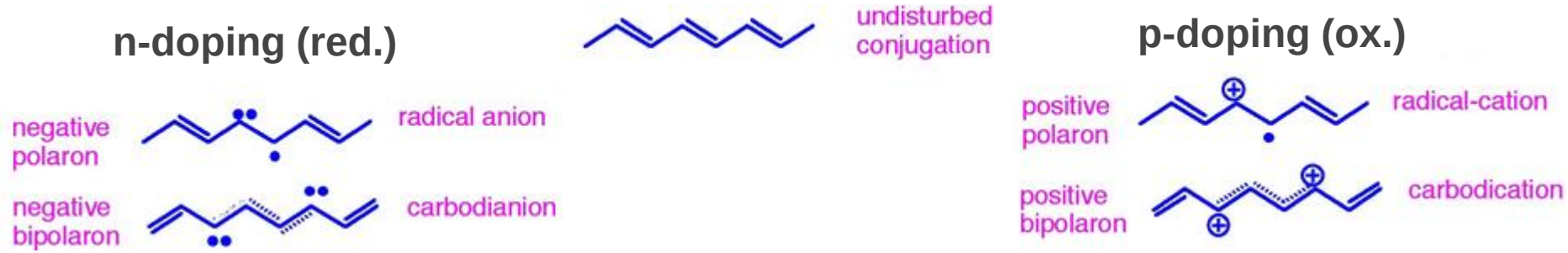

Polaron **(**mobile along the polymer chain).

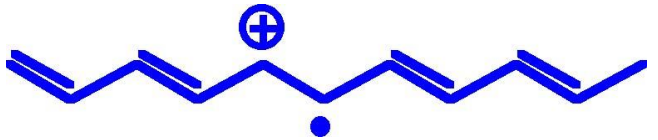

Two polarons may collapse to form a Bipolaron,
(bipolaron are not independent, but move as a pair).

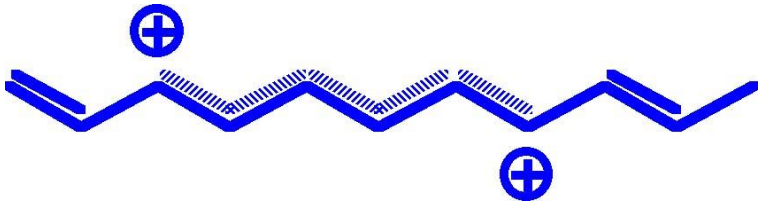

Polyaniline

A conducting polymer that can be grown by using aqueous and non-aqueous route.

Can be obtained by electrochemical synthesis or oxidative coupling of aniline.

Doping achieved by adding protonic acid.

Several forms: leucoemaraldine, emaraldine, emaraldine salt, pernigraniline.

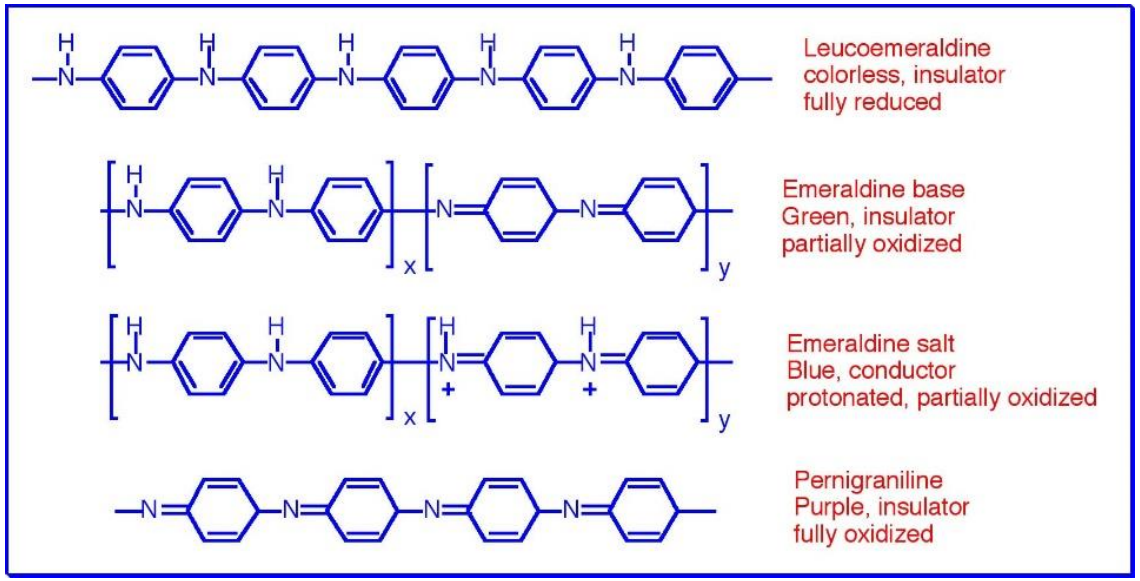

Polythiophene

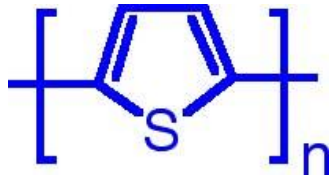

Environmental stable and highly resistant to heat.

Synthesized by the electrochemical polymerization of thiophene.

Can also be obtained by various types of metal catalyzed coupling reaction.

However, the coupling can be either *head-to-head (HH), head-to-tail (HT), or tail-to-tail (TT).*

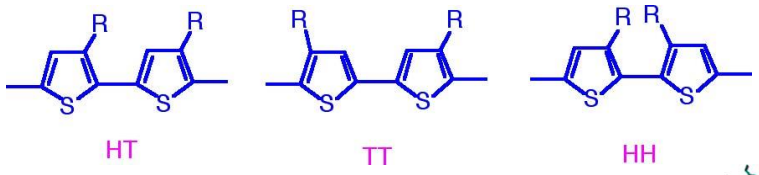

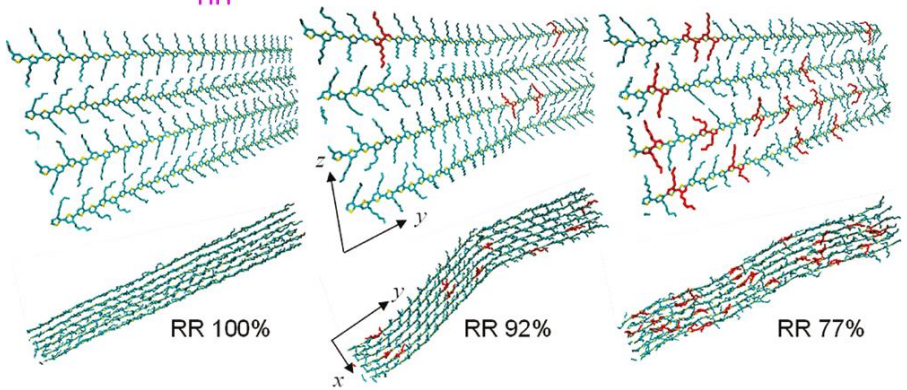

Material	Dopant	s (S cm^{-1})
Polythiophene	$SO_3CF_3^-$	10-20
Poly(3-methylthiophene)	PF_6^-	510
Poly(3-ethylthiophene)	PF_6^-	270
Poly(3-buthylthiophene)	I_2	4
Poly(3-hexylthiophene)	PF_6^-	30
Poly(3-hexylthiophene)	I_2	11

Polymer Conductivity

Typical insulator polymers

- Polyethylene s ~ 10^{-15} S cm^{-1}
- Polytetrafluoroethylene (PTFE) s ~ 10^{-16} S/cm
- Polystyrene s ~ 10^{-15} S/cm

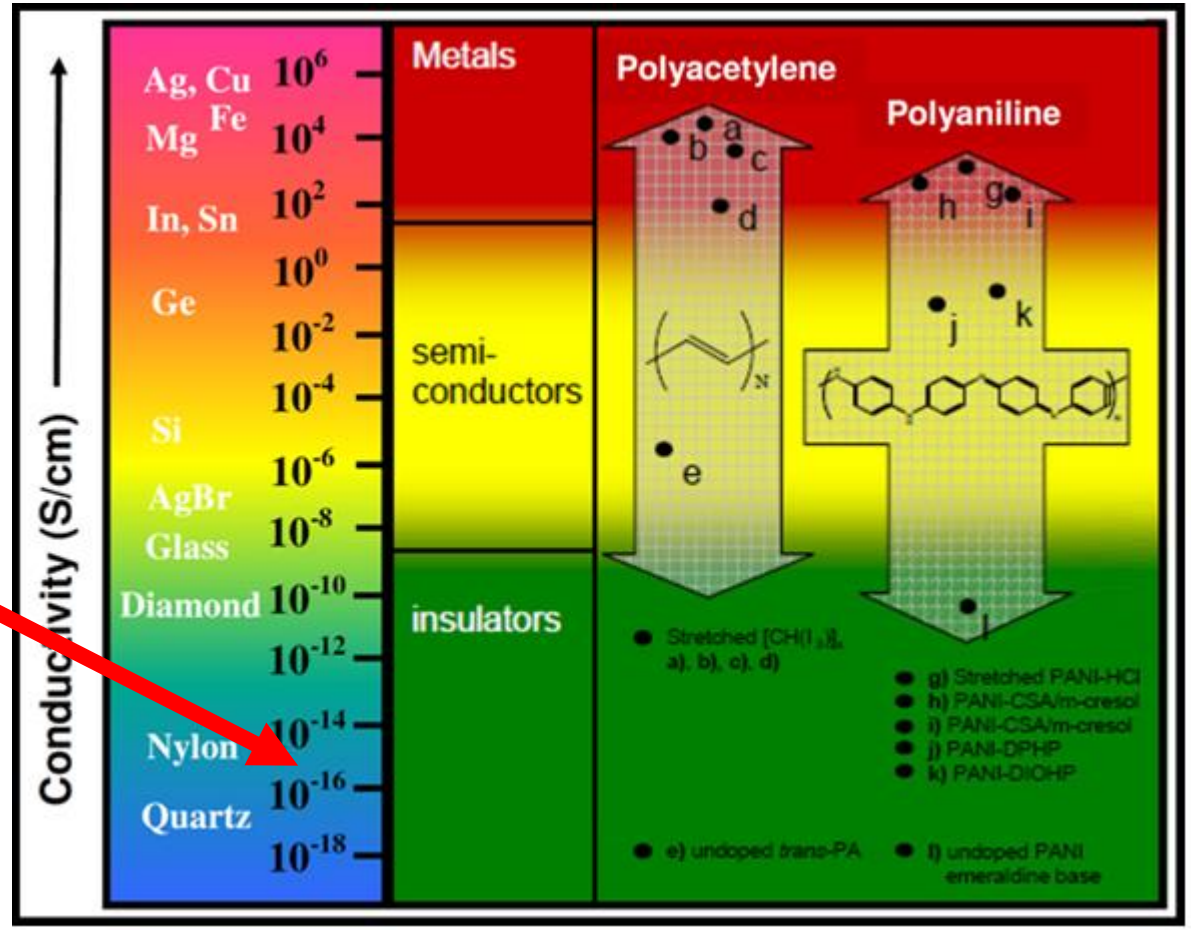

Electrospinning

Process by which high static voltages are used to produce nanometer-scale fibers from a polymer solution.

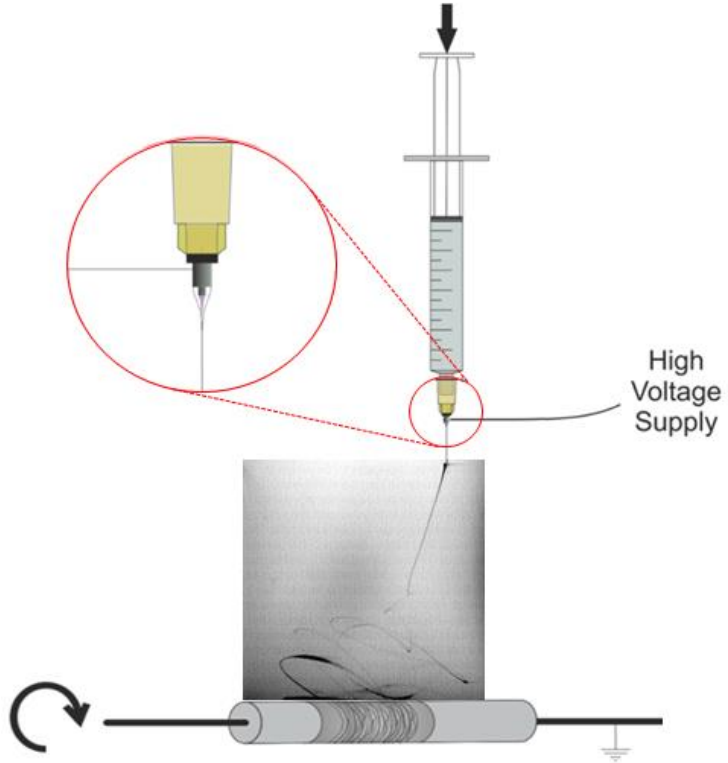

Polymer solution with sufficient molecular weight and viscosity.
High voltages applied to solution.
Fibers deposit on collection target.

Controllable Parameters:

Polymer concentration
Deposition height
Voltage Applied
Flow Rate
Needle Diameter
Temperature/Humidity
Fiber Alignment

Ordered polymer chain structure

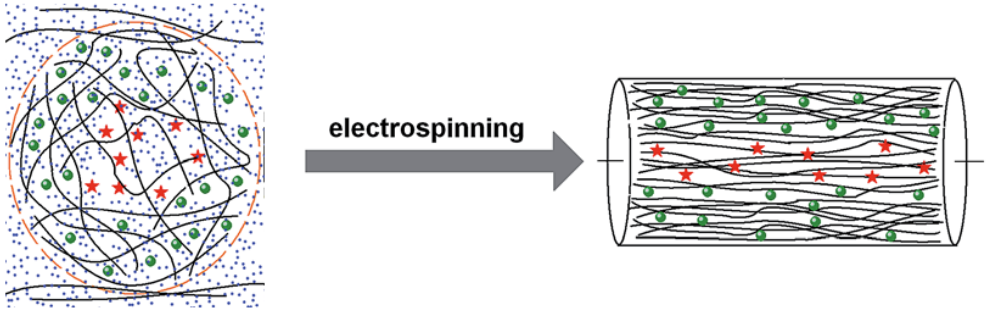

Electrospinning of Polyanyline: pros and cons

Macromolecules — Article — pubs.acs.org/Macromolecules

Electrical Conductivity of Electrospun Polyaniline and Polyaniline-Blend Fibers and Mats

Yuxi Zhang and Gregory C. Rutledge*

Department of Chemical Engineering, Massachusetts Institute of Technology, 77 Massachusetts Avenue, Cambridge, Massachusetts 02139, United States

Advantages

Flexibility and miniaturization

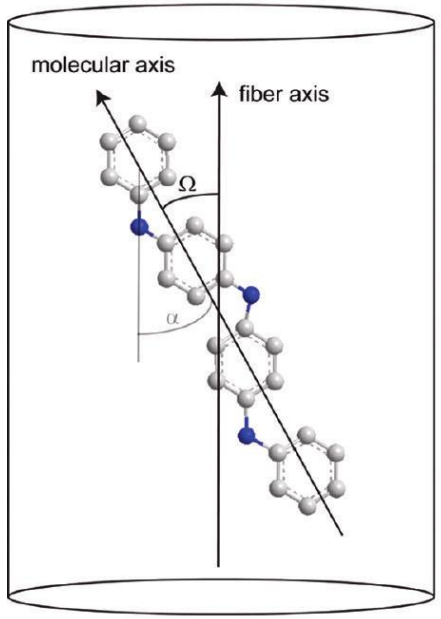

Table 3. Electrical Conductivities of PAni Fibers before and after Stretching

strain	fiber diameter (nm)	electrical conductivity (S/cm)
0	620 ± 160	50 ± 30
0.30	570 ± 200	54 ± 15
0.50	500 ± 150	70 ± 50
0.72	450 ± 70	105 ± 40
1.0	420 ± 130	130 ± 40

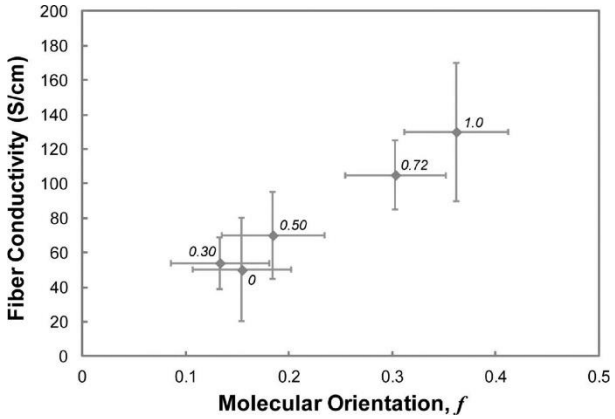

Polymer chain orientation inuced by electrospinning leads to improved electrical properties

Disadvantages

"Blending high molecular weight nonconducting polymers with the conductive polymers to make the solution electrospinnable remains one of the most effective ways to solve the problem of low solution elasticity, the resulting fibers have much lower conductivity due to dilution of the conducting component."

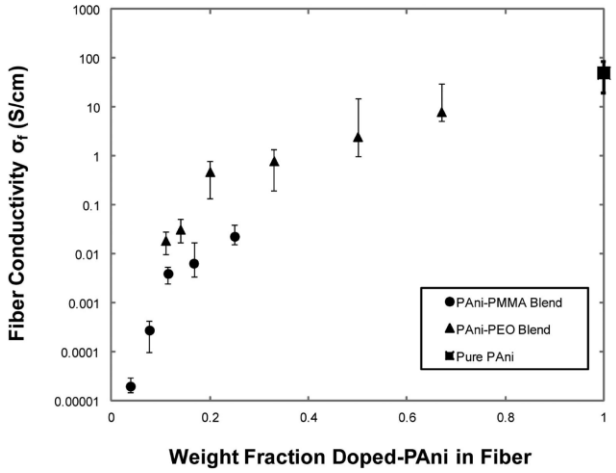

Post-electrospinning nonconducting polymer removal is required to obtain pure PANI nanofiber.

Electrospun Polyaniline-Based Composite Nanofibers

F. Pierini, M. Lanzi, P. Nakielski and T. A. Kowalewski

"*Electrospun polyaniline-based composite nanofibers: tuning the electrical conductivity by tailoring the structure of thiol-protected metal nanoparticles*"

Journal of Nanomaterials, 6142140 (**2017**) 10.

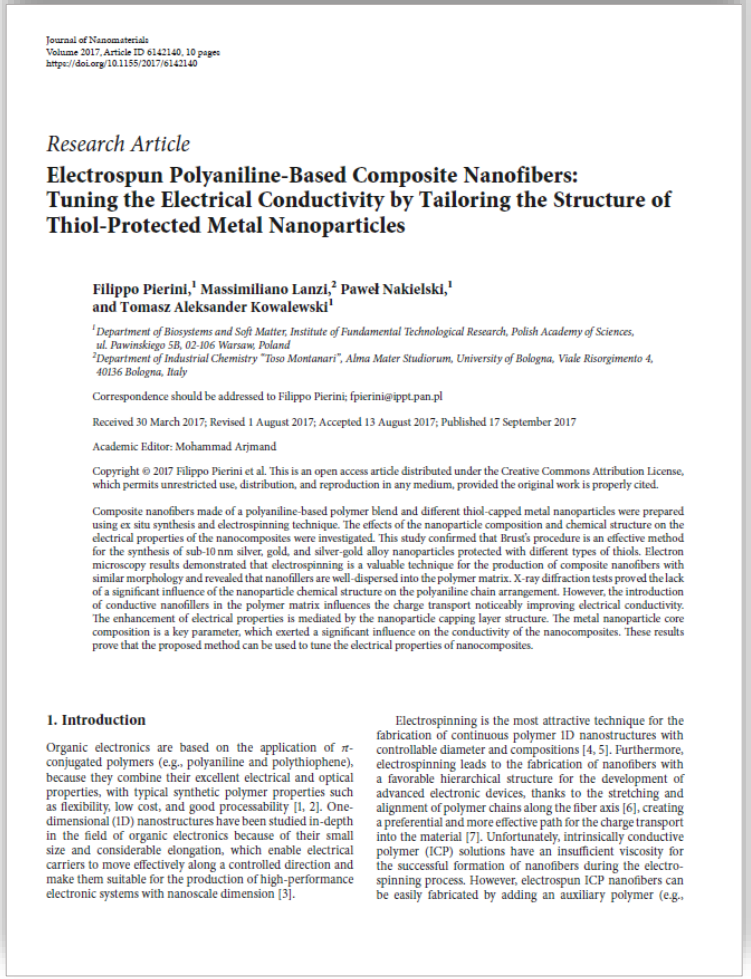

Journal of Nanomaterials
Volume 2017, Article ID 6142140, 10 pages
https://doi.org/10.1155/2017/6142140

Research Article

Electrospun Polyaniline-Based Composite Nanofibers: Tuning the Electrical Conductivity by Tailoring the Structure of Thiol-Protected Metal Nanoparticles

Filippo Pierini,[1] Massimiliano Lanzi,[2] Paweł Nakielski,[1] and Tomasz Aleksander Kowalewski[1]

[1]*Department of Biosystems and Soft Matter, Institute of Fundamental Technological Research, Polish Academy of Sciences, ul. Pawinskiego 5B, 02-106 Warsaw, Poland*
[2]*Department of Industrial Chemistry "Toso Montanari", Alma Mater Studiorum, University of Bologna, Viale Risorgimento 4, 40136 Bologna, Italy*

Correspondence should be addressed to Filippo Pierini; fpierini@ippt.pan.pl

Received 30 March 2017; Revised 1 August 2017; Accepted 13 August 2017; Published 17 September 2017

Academic Editor: Mohammad Arjmand

Composite nanofibers made of a polyaniline-based polymer blend and different thiol-capped metal nanoparticles were prepared using ex situ synthesis and electrospinning technique. The effects of the nanoparticle composition and chemical structure on the electrical properties of the nanocomposites were investigated. This study confirmed that Brust's procedure is an effective method for the synthesis of sub-10 nm silver, gold, and silver-gold alloy nanoparticles protected with different types of thiols. Electron microscopy results demonstrated that electrospinning is a valuable technique for the production of composite nanofibers with similar morphology and revealed that nanofillers are well-dispersed into the polymer matrix. X-ray diffraction tests proved the lack of a significant influence of the nanoparticle chemical structure on the polyaniline chain arrangement. However, the introduction of conductive nanofillers in the polymer matrix influences the charge transport noticeably improving electrical conductivity. The enhancement of electrical properties is mediated by the nanoparticle capping layer structure. The metal nanoparticle core composition is a key parameter, which exerted a significant influence on the conductivity of the nanocomposites. These results prove that the proposed method can be used to tune the electrical properties of nanocomposites.

1. Introduction

Organic electronics are based on the application of π-conjugated polymers (e.g., polyaniline and polythiophene), because they combine their excellent electrical and optical properties, with typical synthetic polymer properties such as flexibility, low cost, and good processability [1, 2]. One-dimensional (1D) nanostructures have been studied in-depth in the field of organic electronics because of their small size and considerable elongation, which enable electrical carriers to move effectively along a controlled direction and make them suitable for the production of high-performance electronic systems with nanoscale dimension [3].

Electrospinning is the most attractive technique for the fabrication of continuous polymer 1D nanostructures with controllable diameter and compositions [4, 5]. Furthermore, electrospinning leads to the fabrication of nanofibers with a favorable hierarchical structure for the development of advanced electronic devices, thanks to the stretching and alignment of polymer chains along the fiber axis [6], creating a preferential and more effective path for the charge transport into the material [7]. Unfortunately, intrinsically conductive polymer (ICP) solutions have an insufficient viscosity for the successful formation of nanofibers during the electrospinning process. However, electrospun ICP nanofibers can be easily fabricated by adding an auxiliary polymer (e.g.,

Electrospinning of Polyanyline

Polymer solution:

500 mg of polyaniline emeraldine base + 645 mg of camphorsulphonic acid + 500 mg of polyethylene oxide in 50 ml of $CHCl_3$

Experimental Paramenters:

Applied electric potential: 9 kV

Distance needle-collector: 15 cm

Flow of polymer solution: 5 µl/min

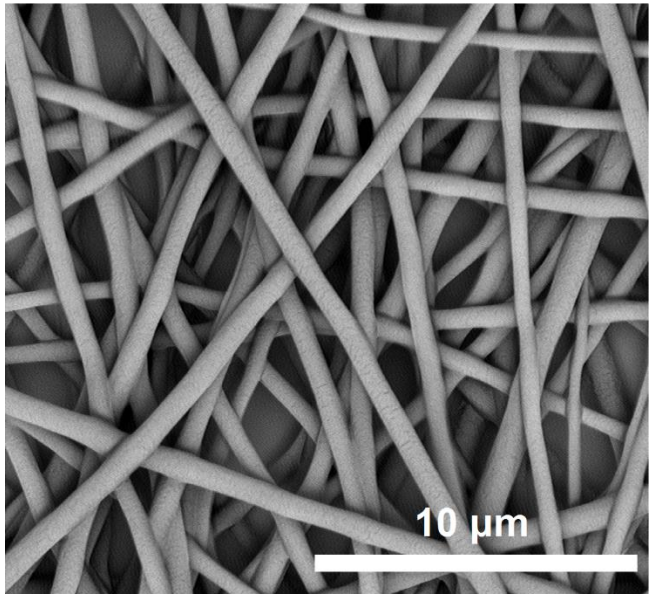

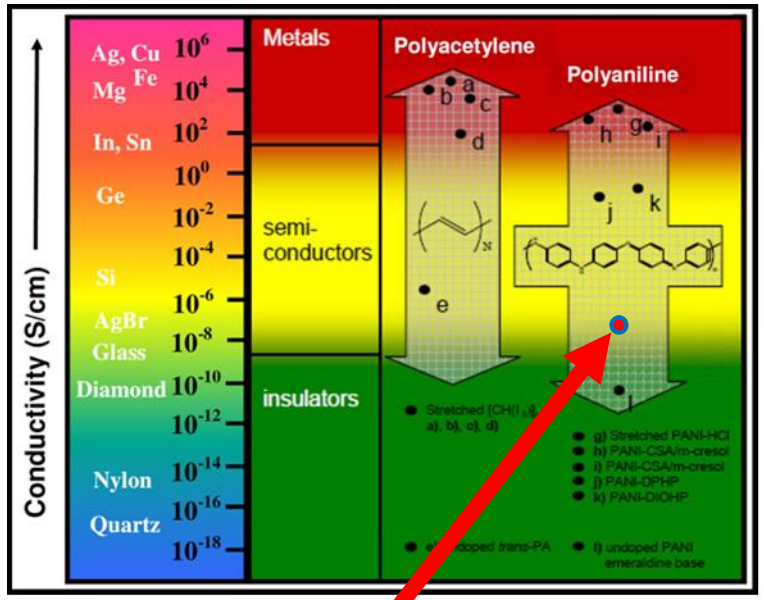

Fiber diameter: 565 ± 75 nm.

Electrical conductivity: $6.81 \times 10^{-8} \pm 3.8 \times 10^{-9}$ S/cm.

Electrospun conductive polymer composites

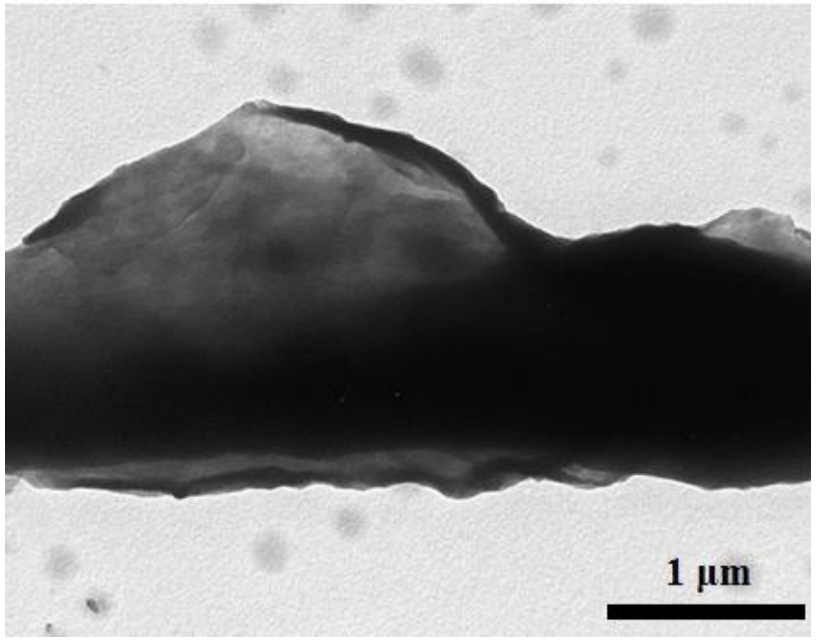

Reduced Graphene Oxide (rGO)

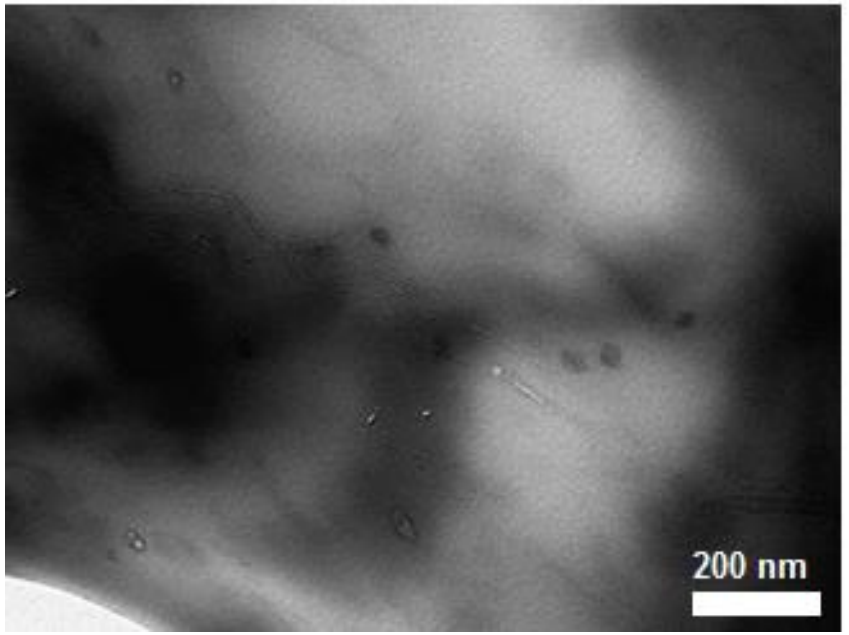

Multi-Walled Carbon Nanotubes (MWCNTs)

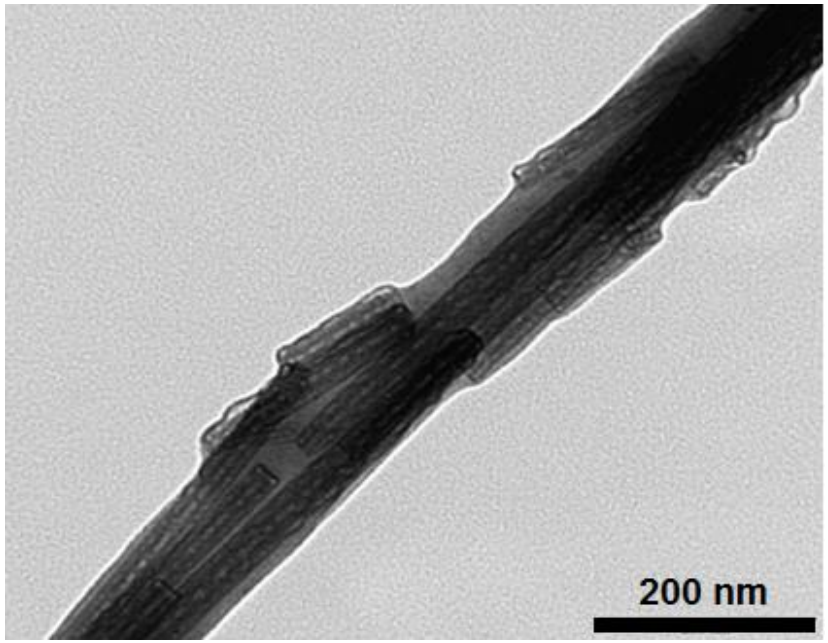

Inorganic Nanotubes

[F. Pierini, M. Lanzi, P. Nakielski, K. Zembrzycki, S. Pawłowska, and T.A. Kowalewski, *"Electrospun poly(3-hexylthiophene)/poly(ethylene oxide)/graphene oxide composite nanofibers: effects of graphene oxide reduction*", Polymers for Advanced Technologies, 27 (**2016**) 1465–1475.]

[F. Pierini, I.G. Lesci, M. Lanzi and N. Roveri, "*Comparison between inorganic geomimetic chrysotile and multiwalled carbon nanotubes for the preparation of one-dimensional conducting polymer nanocomposites*", Fibers and Polymers, 16, (**2015**) 426-433]

Aim

This research is aimed at invastigating proves the possiblity to tailor nanocomposite properties by modifying the chemical structure and surface properties of nanofillers without changing the polymer blend composition and the nanofiller concentration.

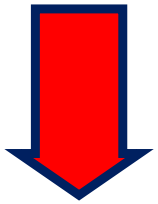

Several material properties should be maintened unchanged:

- Nanofiber dimension and orientation
- Polymer structure (e.g. crystallinity)
- Nanofiller dimension, concentration and geometrical distribution

Electrospun Polyaniline-metal nanoparticle composites

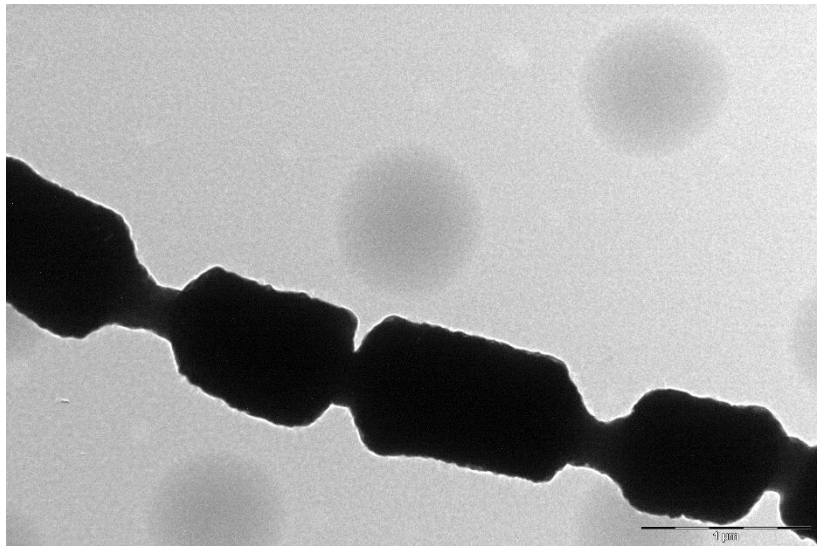

Electrospun Polyaniline and Silver nanoparticles fibers

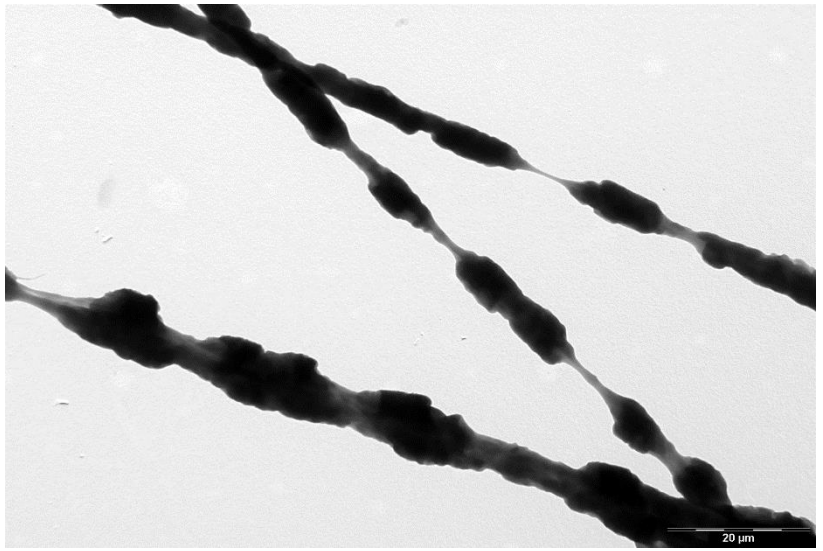

Electrospun Polyaniline and Copper nanoparticles fibers

Kiełbasa-like structure

Thiol-protected metal nanoparticles

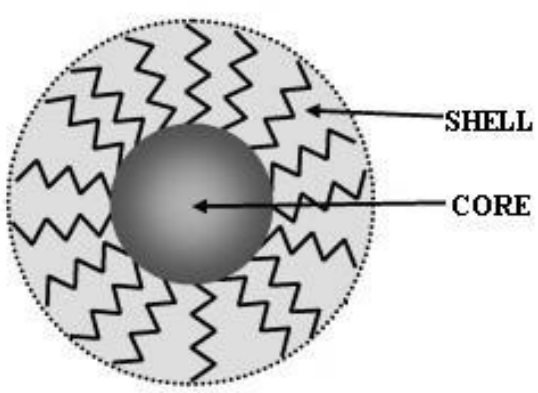

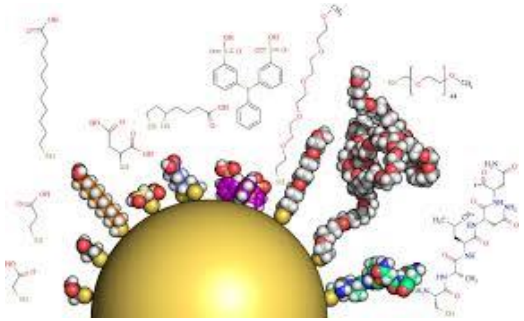

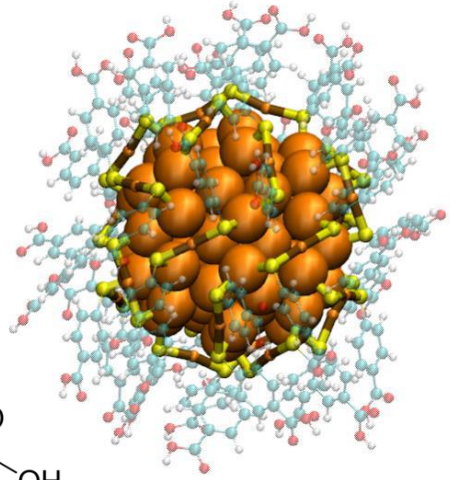

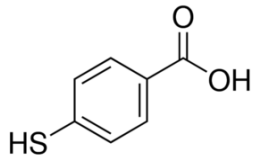

p-mercaptobenzoic acid

Advantages:

- stable without aggregation
- possibility to attach several kind of molecules

Disadvantages:

- non-conductive shell

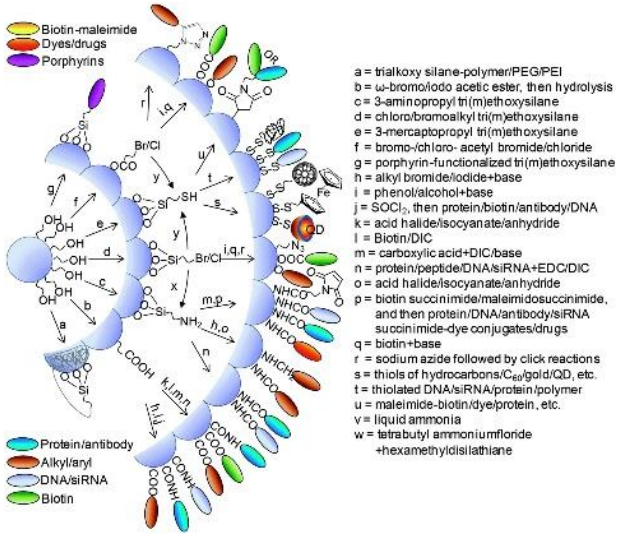

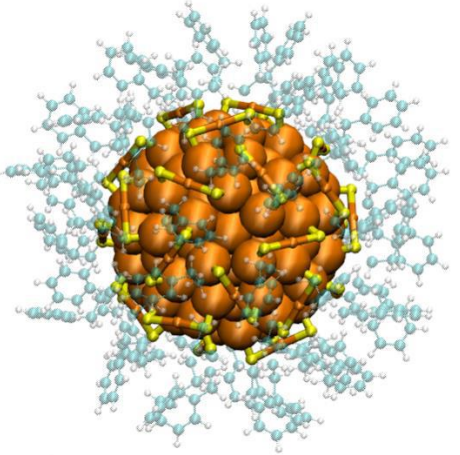

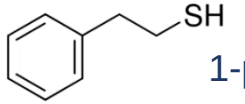

1-phenylethyl mercaptan

Ag Nanoparticles

Brust–Schiffrin synthesis (BSS)

Nitrogen atmosphere
Room Temperature

1,0 mmol of $AgNO_3$
2,4 mmol of NaBr in 30 ml H_2O
1,85 mmol of TOABr in 20 ml of toluene
3,1 mmol of BuSH in 30 ml of toluene

} SHAKE FOR 30' AND PHASE SEPARATION

10 mmol of $NaBH_4$ in 15 ml of H_2O mQ

} SHAKE FOR 3h AND PHASE SEPARATION

Solvent evaporation
Washing with methanol
Final solvent: methanol

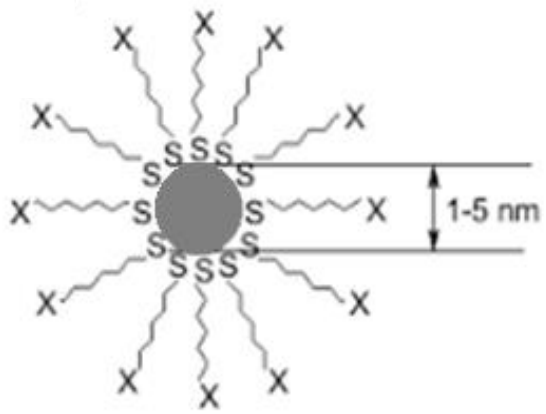

Thiol-protected metal nanoparticles

Metal core composition

Nanoparticles	Starting metal salt	Capping agent
Au-MBT	0.5 mmol of $HAuCl_4$	1 mmol of MBT
Au_4Ag_1-MBT	0.4 mmol of $HAuCl_4$ + 0.1 mmol of $AgNO_3$	1 mmol of MBT
Au_1Ag_4-MBT	0.1 mmol of $HAuCl_4$ + 0.4 mmol of $AgNO_3$	1 mmol of MBT
Ag-MBT	0.5 mmol of $AgNO_3$	1 mmol of MBT
Ag-BuT	0.5 mmol of $AgNO_3$	1 mmol of BuT

Organic shell structure

Capping agents

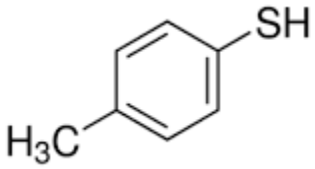

4-methylbenzenethiol (MBT)

Butanethiol (BuT)

Thiol-protected metal nanoparticles

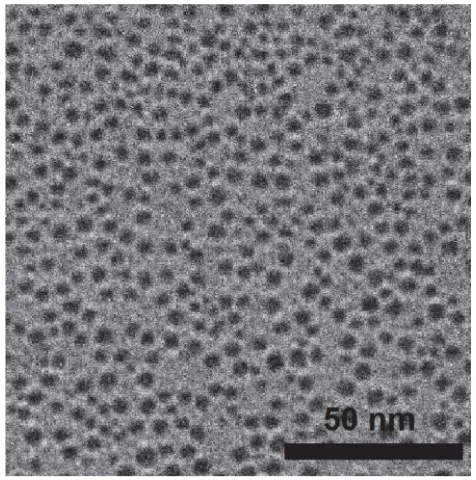

Ag-BuT

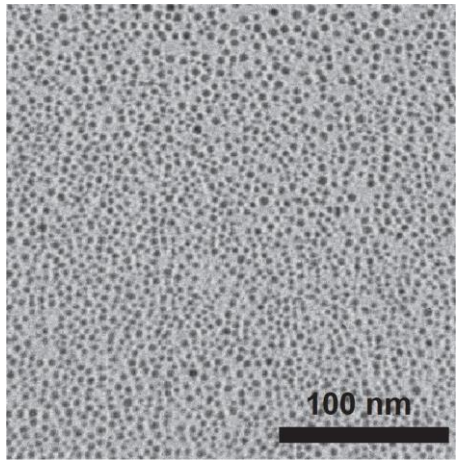

Ag-MBT

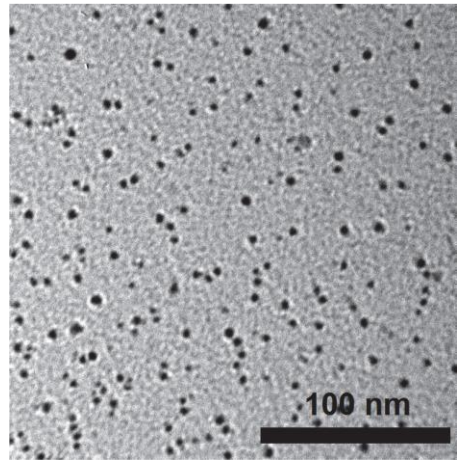

Au-MBT

Spherical
5/6 nm particles.

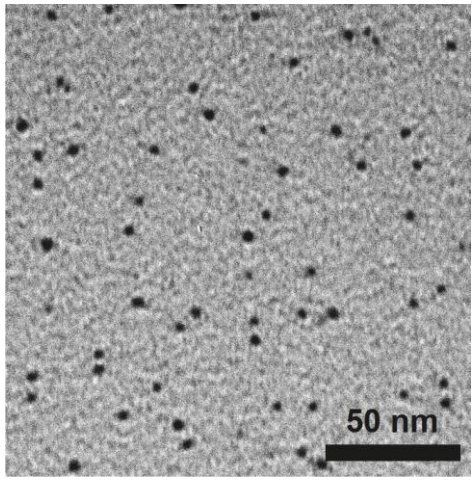

Au_4Ag_1-MBT

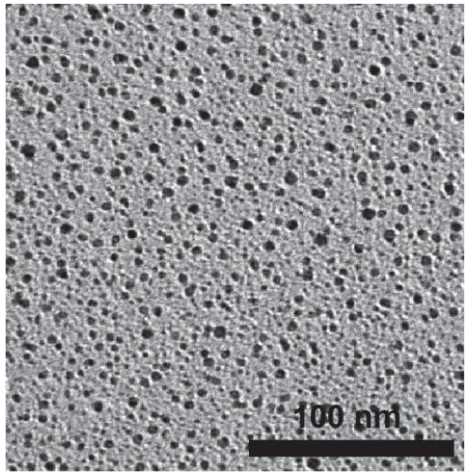

Au_1Ag_4-MBT

Thiol-protected metal nanoparticles

Journal of Materials Chemistry B

PAPER View Article Online View Journal | View Issue

Cite this: J. Mater. Chem. B, 2015, 3, 4654

Nanostructure of wet-chemically prepared, polymer-stabilized silver–gold nanoalloys (6 nm) over the entire composition range

S. Ristig,[a] O. Prymak,[a] K. Loza,[a] M. Gocyla,[b] W. Meyer-Zaika,[a] M. Heggen,[b] D. Raabe[c] and M. Epple*[a]

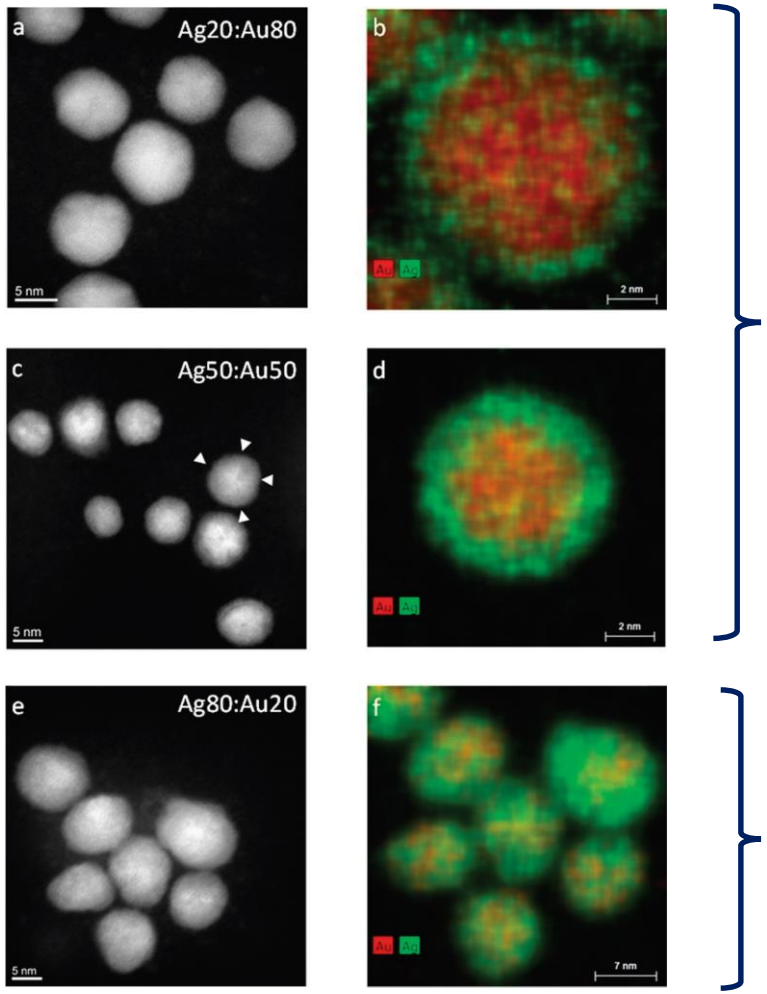

Scanning transmission electron microscopy (STEM) combined with

energy-dispersive X-ray spectroscopy (EDX)

Capped AuAg alloy nanoparticles have a metal core-shell structure with an Au-rich core and an Ag-rich shell at a low silver content.

When the amount of silver is predominant, the distribution of metals into the nanoalloys structure is stochastic and a single particle contains more than one crystallite. The different size distribution of Au_1Ag_4-MBT results from a change in the nucleation and growth mechanism if compared with the other nanoparticles.

Metal core composition

UV-Vis

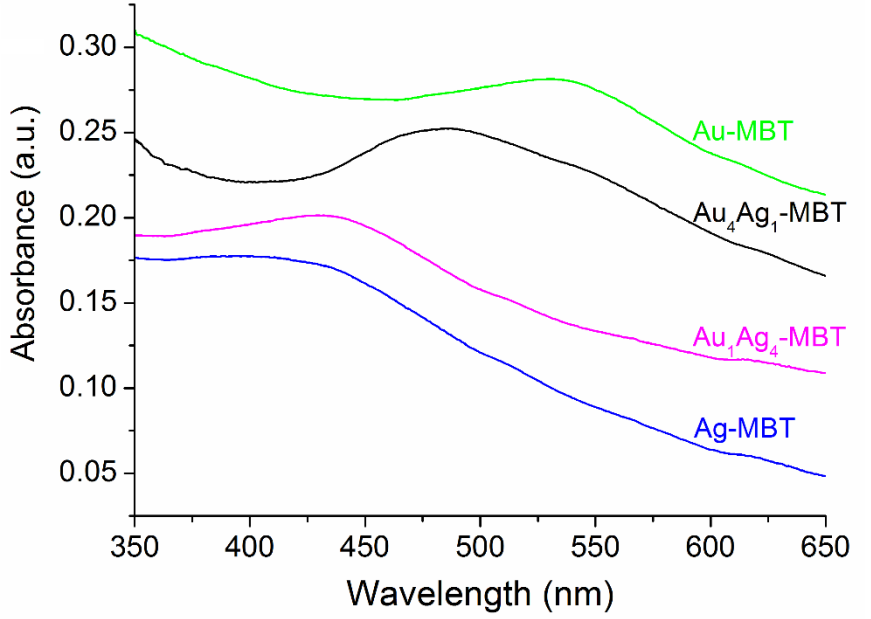

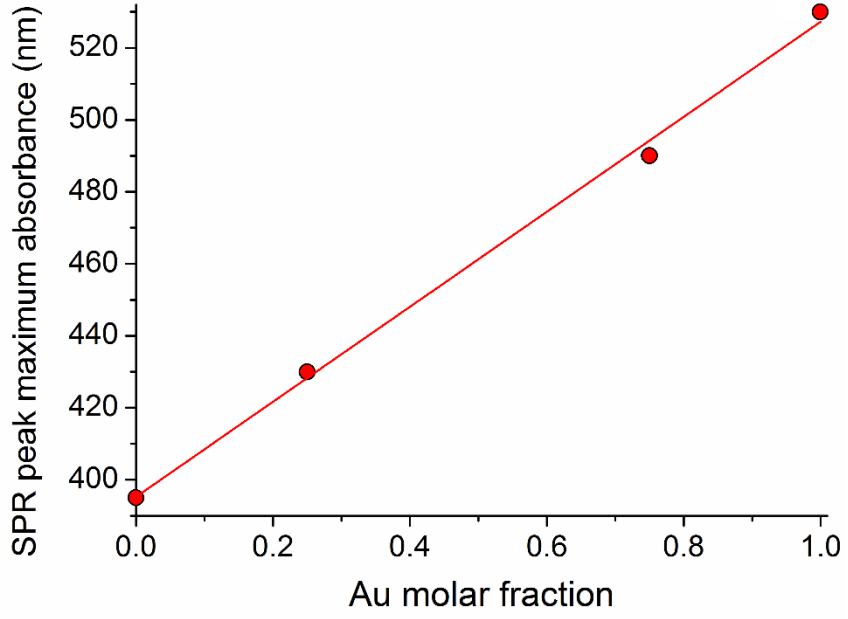

Capped metal nanoparticles show surface plasmon resonance (SPR), due to the interaction between light and metal electrons in the conduction band which collectively oscillate in resonance at specific wavelength. SPR wavelength varies with particle size, shape, and metal type.

The continuous change in the SPR absorption maximum as a function of the Au : Ag molar ratio can be used to accurately quantify the composition of alloy nanoparticles.

Organic shell composition

FT-IR

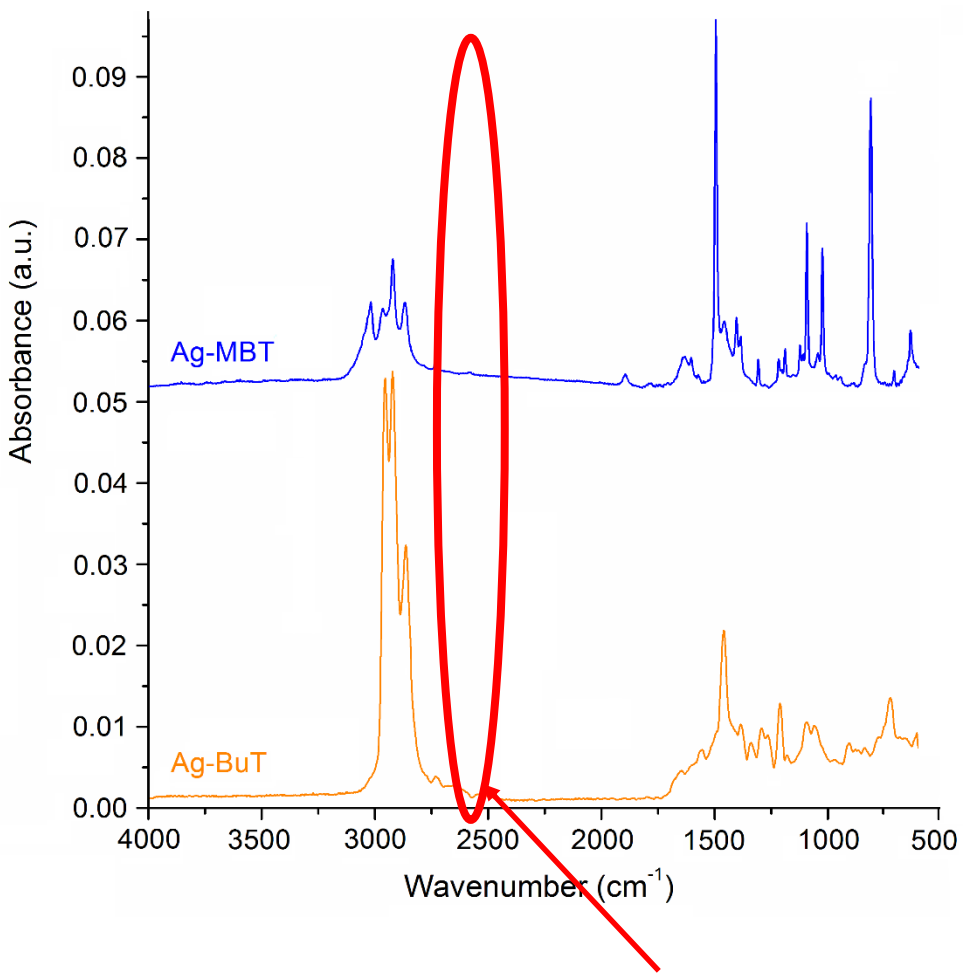

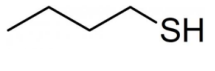

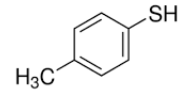

Assignments	Ag-BuT (cm^{-1})	Ag-MBT (cm^{-1})
ν =CH (aromatic group)	-	3015
ν $-CH_3$ (alkyl group)	2956	2850 - 3000
$\nu_{asymmetric}$ $-CH_2$ (alkyl group)	2932	-
$\nu_{symmetric}$ $-CH_2$ (alkyl group)	2685	-
ν C-C=C (aromatic group)	-	1400 - 1650
γ $-CH_2$ (alkyl group)	1460	-
$\gamma_{in\text{-}plane}$ =CH (aromatic group)	-	1000 - 1200
$\gamma_{out\text{-}of\text{-}plane}$ =CH (aromatic group)	-	801

ν S-H (thiol group) 2550-2600 cm^{-1}

Organic shell composition

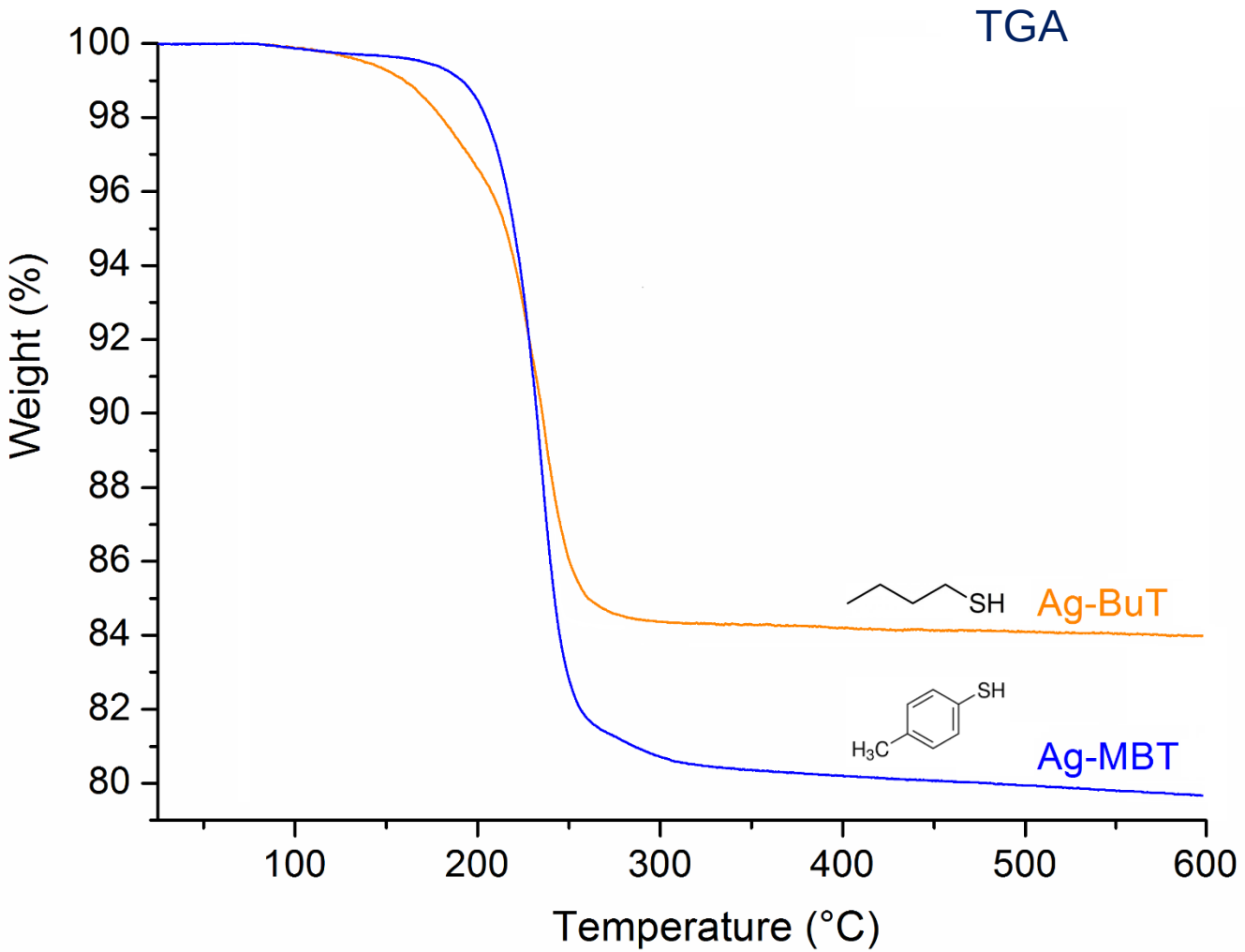

The total mass loss for of Ag-BuT is almost 16%, while total mass loss for Ag-MBT is more than 20%, which is consistent with the molecular mass of the capping agents. This, confirms that the number of thiol molecules attached onto the metal surface is comparable.

The Ag-BuT degradation took place in a wider range of temperature swhich is an indicator of the degree of disorder in interchain interactions, especially when compared with Ag-MBT nanoparticles where the π–π stacking of aromatic rings can create stable supramolecular structures.

Electrospun composite nanofibers

Polyaniline (500 mg) + HSCA (645 mg) + PEO (500 mg) dissolved in 50 ml of $CHCl_3$

5.0 mg of nanoparticles (7.06 wt% of the final dry composite) to 2.0 ml of polymer blend solution.

Sample	Solution flow rate (μl/min)	Applied voltage (kV)	Needle-target distance (cm)
Neat nanofibers	5.0	9.0	15.0
PANI/Au-MBT	5.0	8.0	12.0
PANI/Au_4Ag_1-MBT	5.0	7.0	10.0
PANI/Au_1Ag_4-MBT	5.0	7.0	10.0
PANI/Ag-MBT	5.0	8.0	8.0
PANI/Ag-BuT	5.0	8.0	8.0

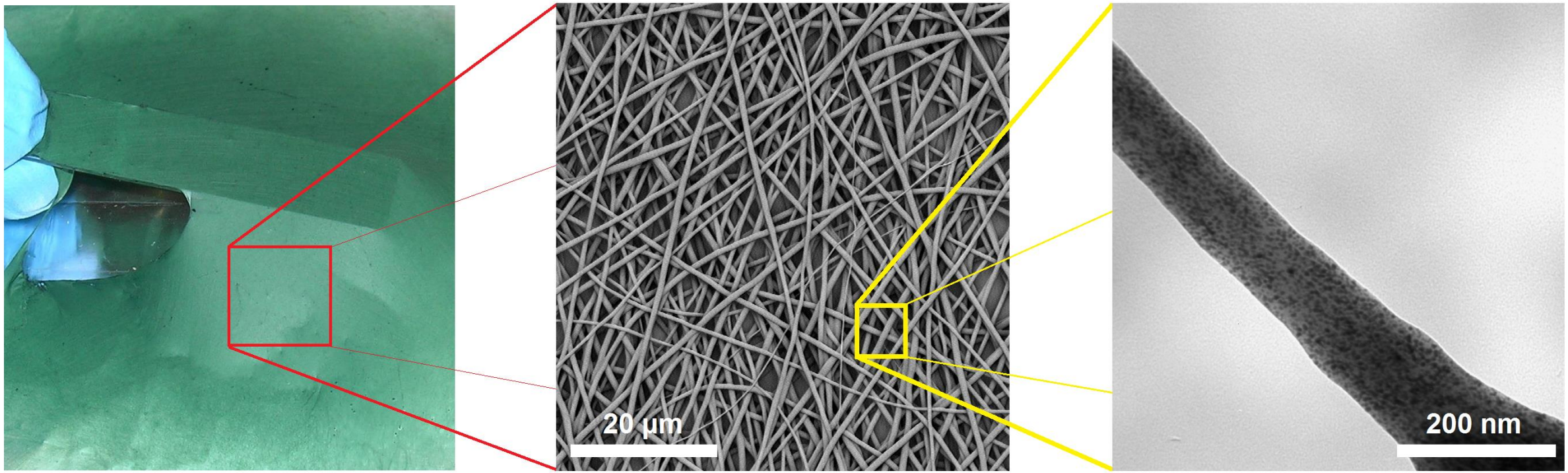

Electrospun composite nanofibers: morphology

SEM

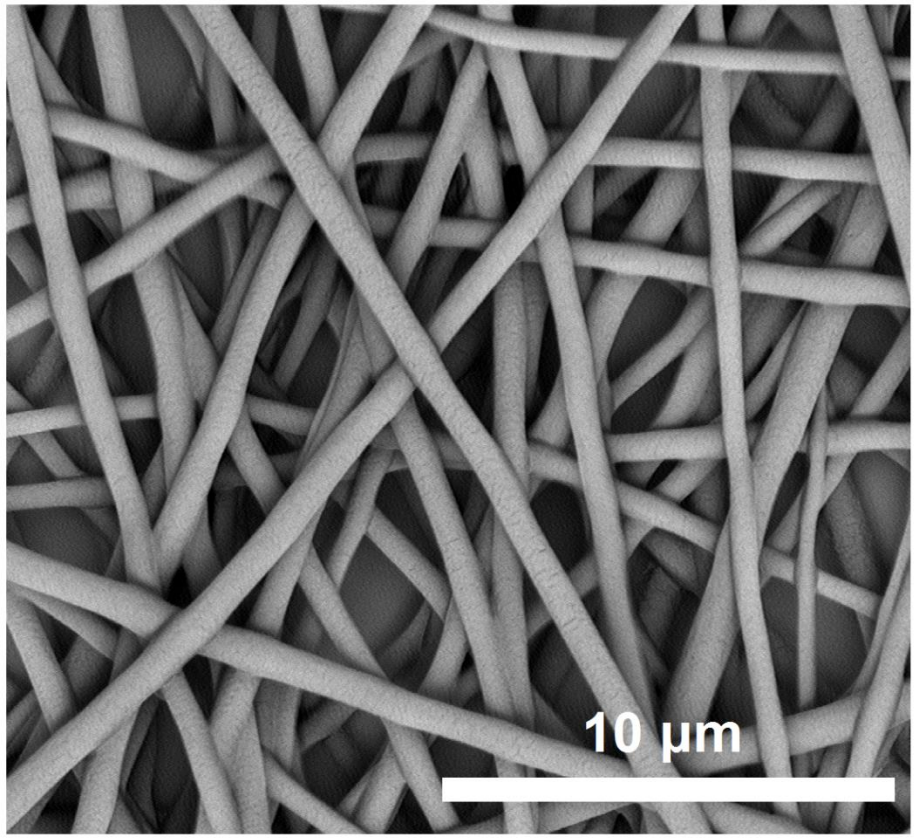

PANI nanofibers

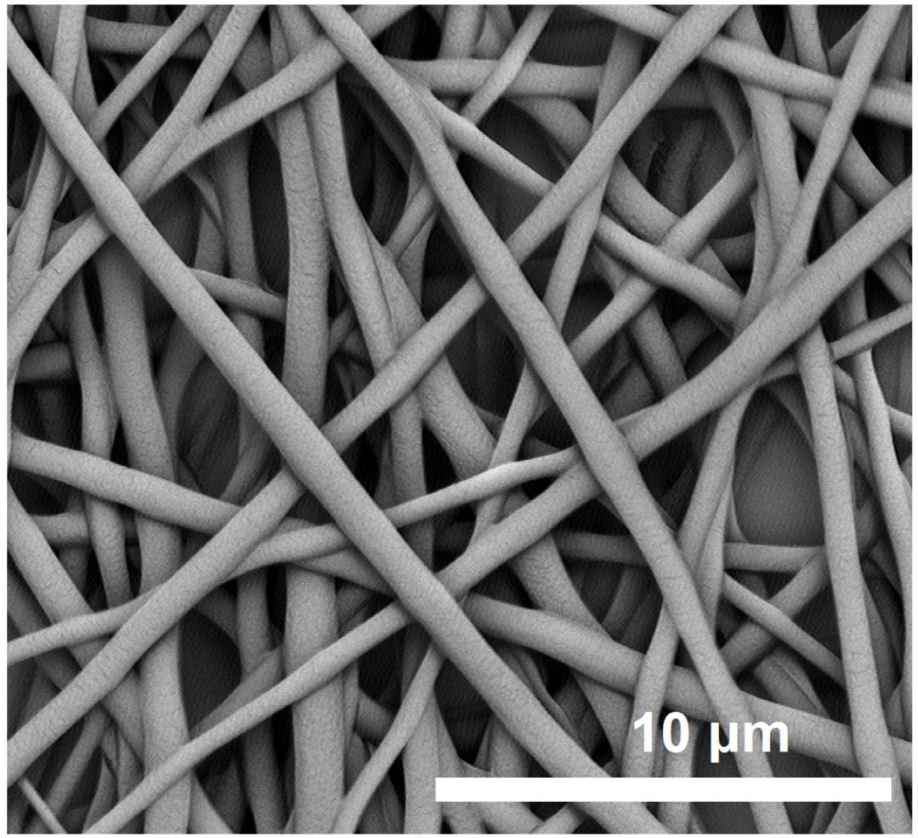

PANI/Ag-MBT nanofibers

Electrospun composite nanofibers: morphology

TEM

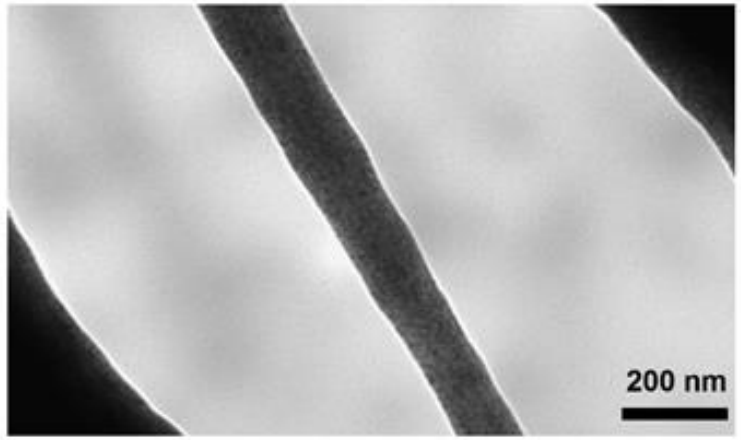

PANI/Ag-BuT nanofibers

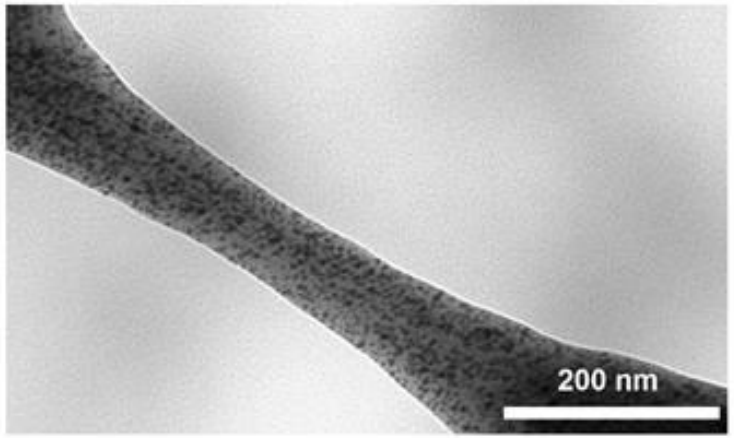

PANI/Ag-MBT nanofibers

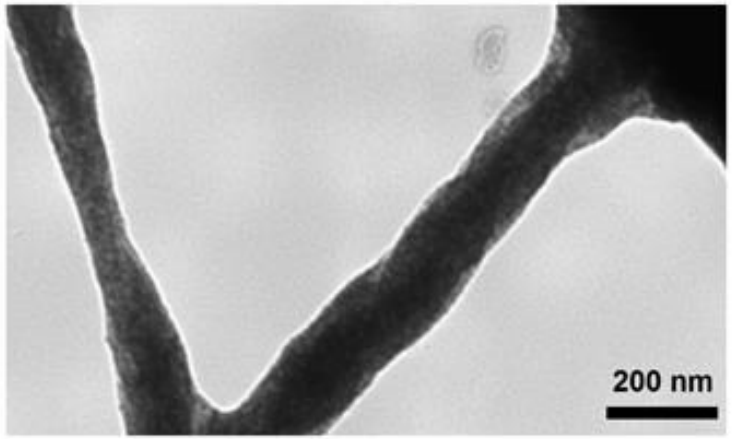

PANI/Au-MBT nanofibers

PANI/Au_4Ag_1-MBT nanofibers

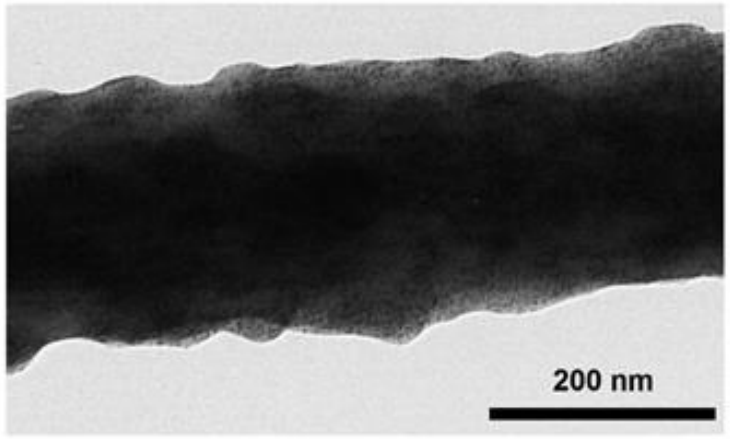

PANI/Au_1Ag_4-MBT nanofibers

Electrospun composite nanofibers: chemical structure

XRD

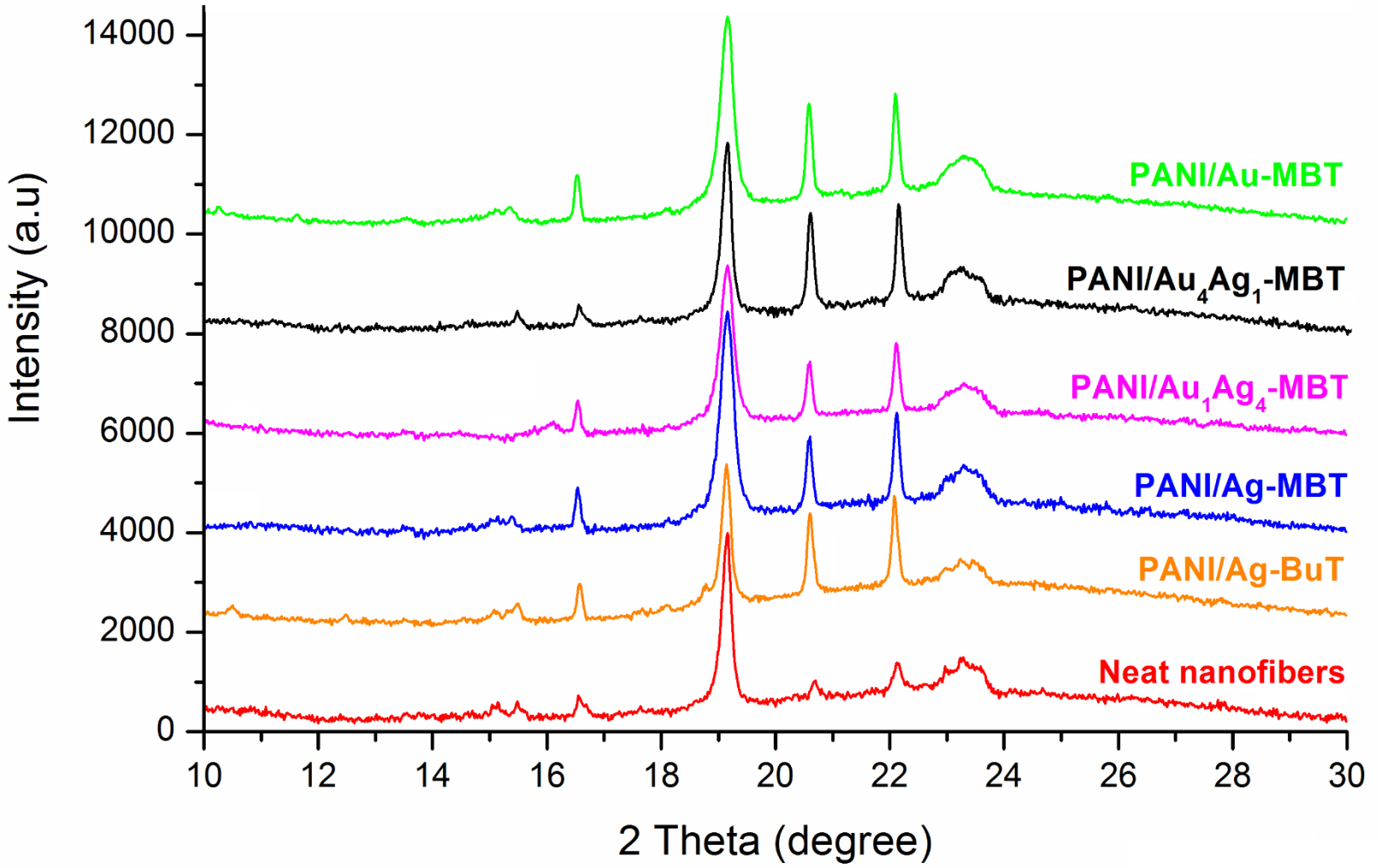

Two typical peaks at 2θ = 19.1º and 23.3º, which correspond to semicrystalline PEO.

Crystalline PANI peak diffracted at an angle of 2θ=25.72° is absent.

Electrospun nanofibers: electrical properties

Four Point Probe Test

Nanoparticle metal core influence

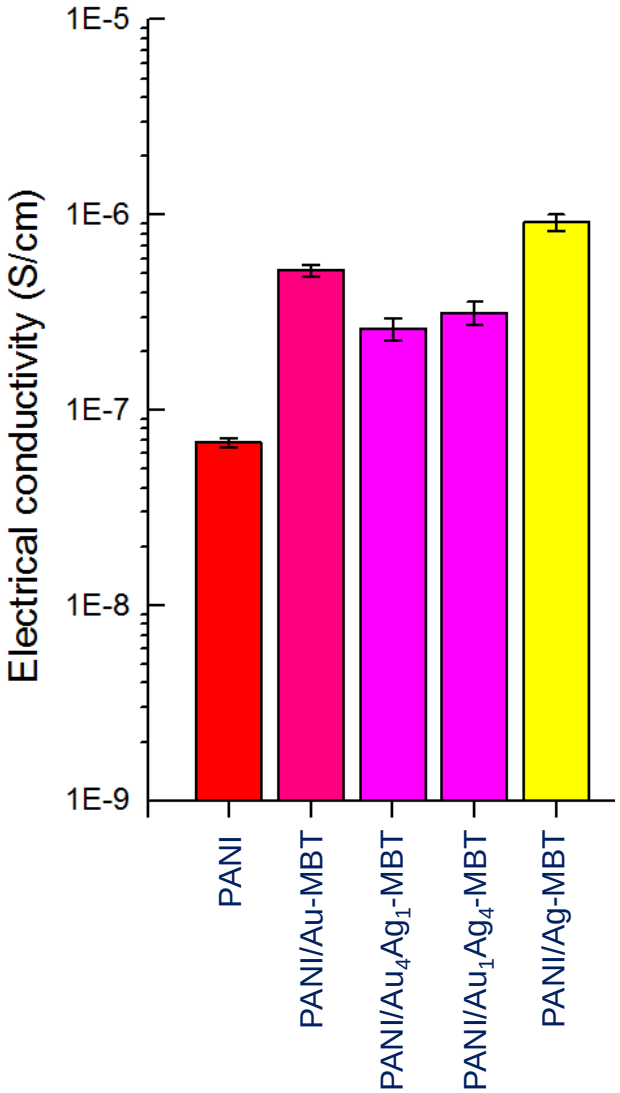

Sample	Fiber diameter (nm)	Electrical conductivity (S/cm)
PANI	565 ± 75	$6.81 \times 10^{-8} \pm 3.8 \times 10^{-9}$
PANI/Au-MBT	635 ± 135	$5.20 \times 10^{-7} \pm 3.6 \times 10^{-8}$
PANI/Au_4Ag_1-MBT	690 ± 116	$2.61 \times 10^{-7} \pm 3.4 \times 10^{-8}$
PANI/Au_1Ag_4-MBT	678 ± 127	$3.16 \times 10^{-7} \pm 4.2 \times 10^{-8}$
PANI/Ag-MBT	648 ± 109	$9.18 \times 10^{-7} \pm 8.5 \times 10^{-8}$
PANI/Ag-BuT	611 ± 101	$3.19 \times 10^{-6} \pm 2.9 \times 10^{-7}$

Nanoparticle organic shell influence

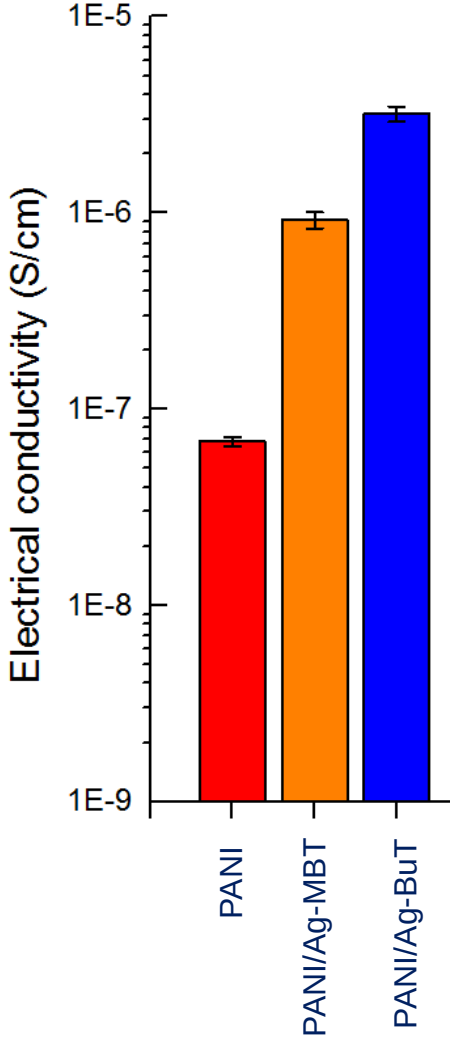

Electrospun Polyaniline-Based Composite Nanofibers: Conclusions

- Nanofibers have defect-free cylindrical morphology, with similar fiber diameter and orientation.

- Uniform dispersion of the spherically shaped metal nanoparticles in all the electrospun polymer nanofibers.

- Conjugated polymer chain arrangement is not affected by the presence of nanofillers.

- Polymer matrix structure is not influenced by the metal nanoparticle core and thiol protecting layer composition.

- Nanocomposites exhibit improved electrical conductivity when compared with the electrospun neat material.

- The electrical conductivity of electrospun nanocomposites is influenced by the nanoparticle metal core composition and structure.

- Pivotal role of the thiol layer structure in order to produce nanocomposites with desirable electrical properties.

Electrospun Nanofibers for Organic Photovoltaics

F. Pierini, M. Lanzi, P. Nakielski, S. Pawłowska, O. Urbanek, K. Zembrzycki and T.A. Kowalewski

"*Single-material organic solar cells based on electrospun fullerene-grafted polythiophene nanofibers"*

Macromolecules, 50, 13 (**2017**) 4972-4981.

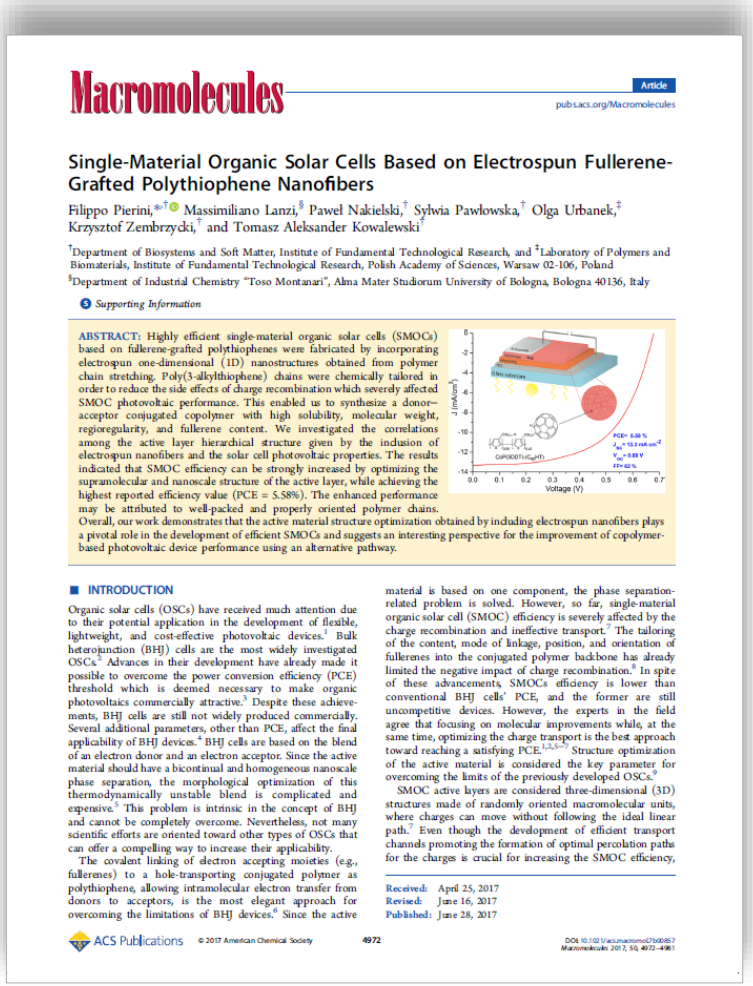

Macromolecules

Article

pubs.acs.org/Macromolecules

Single-Material Organic Solar Cells Based on Electrospun Fullerene-Grafted Polythiophene Nanofibers

Filippo Pierini,*[†] Massimiliano Lanzi,[§] Paweł Nakielski,[†] Sylwia Pawłowska,[†] Olga Urbanek,[‡] Krzysztof Zembrzycki,[†] and Tomasz Aleksander Kowalewski[†]

[†]Department of Biosystems and Soft Matter, Institute of Fundamental Technological Research, and [‡]Laboratory of Polymers and Biomaterials, Institute of Fundamental Technological Research, Polish Academy of Sciences, Warsaw 02-106, Poland

[§]Department of Industrial Chemistry "Toso Montanari", Alma Mater Studiorum University of Bologna, Bologna 40136, Italy

Supporting Information

ABSTRACT: Highly efficient single-material organic solar cells (SMOCs) based on fullerene-grafted polythiophenes were fabricated by incorporating electrospun one-dimensional (1D) nanostructures obtained from polymer chain stretching. Poly(3-allylthiophene) chains were chemically tailored in order to reduce the side effects of charge recombination which severely affected SMOC photovoltaic performance. This enabled us to synthesize a donor−acceptor conjugated copolymer with high solubility, molecular weight, regioregularity, and fullerene content. We investigated the correlations among the active layer hierarchical structure given by the inclusion of electrospun nanofibers and the solar cell photovoltaic properties. The results indicated that SMOC efficiency can be strongly increased by optimizing the supramolecular and nanoscale structure of the active layer, while achieving the highest reported efficiency value (PCE = 5.58%). The enhanced performance may be attributed to well-packed and properly oriented polymer chains. Overall, our work demonstrates that the active material structure optimization obtained by including electrospun nanofibers plays a pivotal role in the development of efficient SMOCs and suggests an interesting perspective for the improvement of copolymer-based photovoltaic device performance using an alternative pathway.

INTRODUCTION

Organic solar cells (OSCs) have received much attention due to their potential application in the development of flexible, lightweight, and cost-effective photovoltaic devices.[1] Bulk heterojunction (BHJ) cells are the most widely investigated OSCs.[2] Advances in their development have already made it possible to overcome the power conversion efficiency (PCE) threshold which is deemed necessary to make organic photovoltaics commercially attractive.[3] Despite these achievements, BHJ cells are still not widely produced commercially. Several additional parameters, other than PCE, affect the final applicability of BHJ devices.[4] BHJ cells are based on the blend of an electron donor and an electron acceptor. Since the active material should have a bicontinual and homogeneous nanoscale phase separation, the morphological optimization of this thermodynamically unstable blend is complicated and expensive.[5] This problem is intrinsic in the concept of BHJ and cannot be completely overcome. Nevertheless, not many scientific efforts are oriented toward other types of OSCs that can offer a compelling way to increase their applicability.

The covalent linking of electron accepting moieties (e.g., fullerenes) to a hole-transporting conjugated polymer as polythiophene, allowing intramolecular electron transfer from donors to acceptors, is the most elegant approach for overcoming the limitations of BHJ devices.[6] Since the active material is based on one component, the phase separation-related problem is solved. However, so far, single-material organic solar cell (SMOC) efficiency is severely affected by the charge recombination and ineffective transport.[7] The tailoring of the content, mode of linkage, position, and orientation of fullerenes into the conjugated polymer backbone has already limited the negative impact of charge recombination.[8] In spite of these advancements, SMOCs efficiency is lower than conventional BHJ cells' PCE, and the former are still uncompetitive devices. However, the experts in the field agree that focusing on molecular improvements while, at the same time, optimizing the charge transport is the best approach toward reaching a satisfying PCE.[1,2,5−7] Structure optimization of the active material is considered the key parameter for overcoming the limits of the previously developed OSCs.[9]

SMOC active layers are considered three-dimensional (3D) structures made of randomly oriented macromolecular units, where charges can move without following the ideal linear path.[7] Even though the development of efficient transport channels promoting the formation of optimal percolation paths for the charges is crucial for increasing the SMOC efficiency,

Received: April 25, 2017
Revised: June 16, 2017
Published: June 28, 2017

Photovoltaics

Organic solar cell disadvantages:

- lower performance
- instability

Why “ORGANIC“?

Advantages:

- light weight
- flexible
- low cost
- large area
- -“tailor-made“ properties

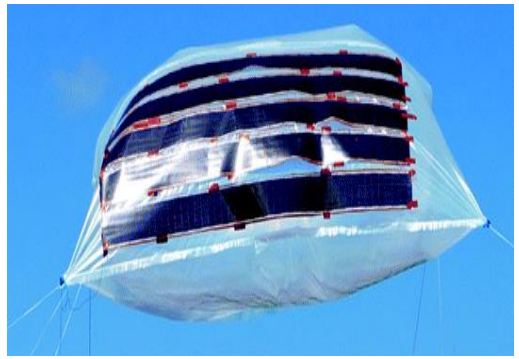

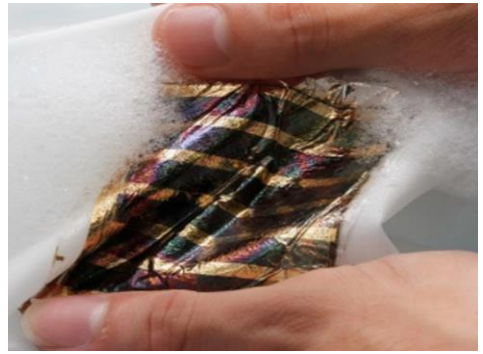

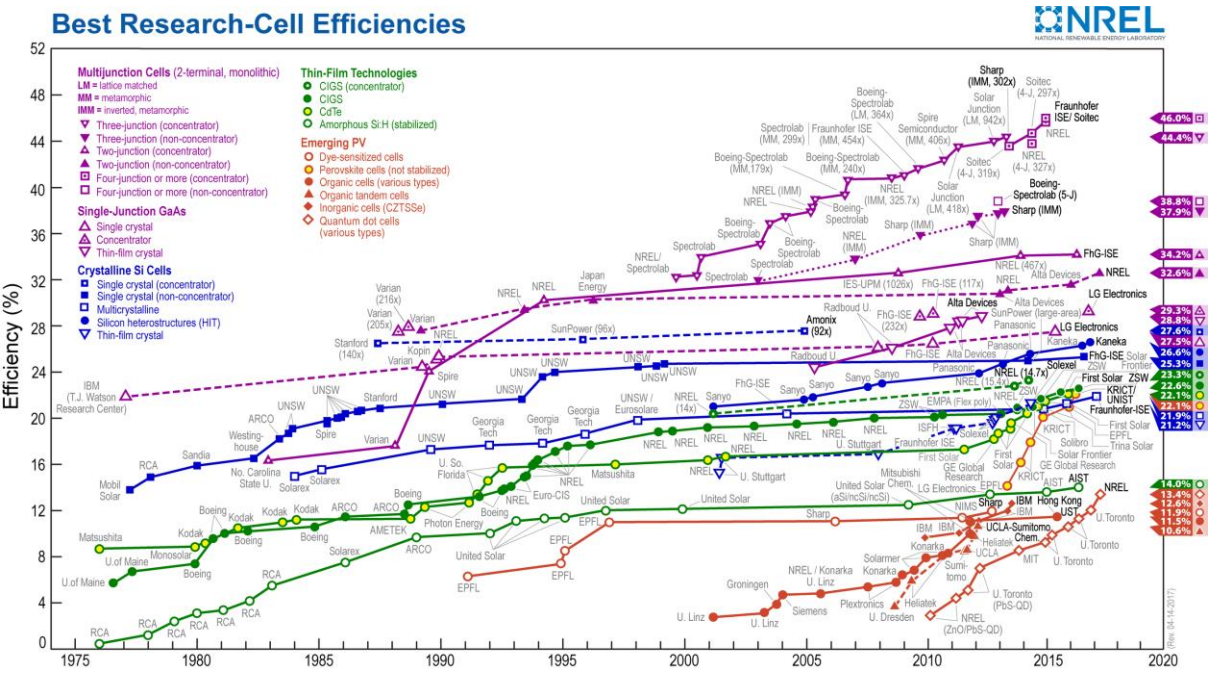

Organic solar cells

Flexible and light weight

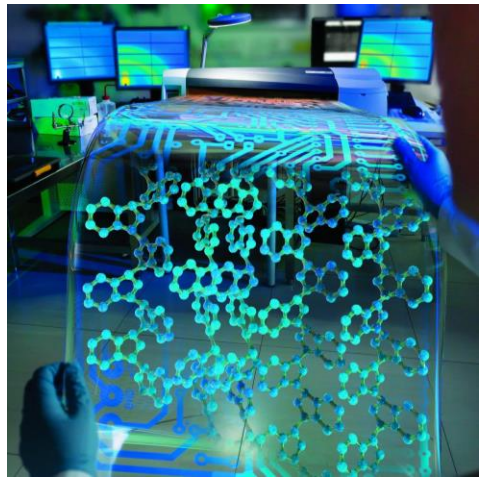

Printable

The Role of Electrospinning in the Emerging Photovoltaics

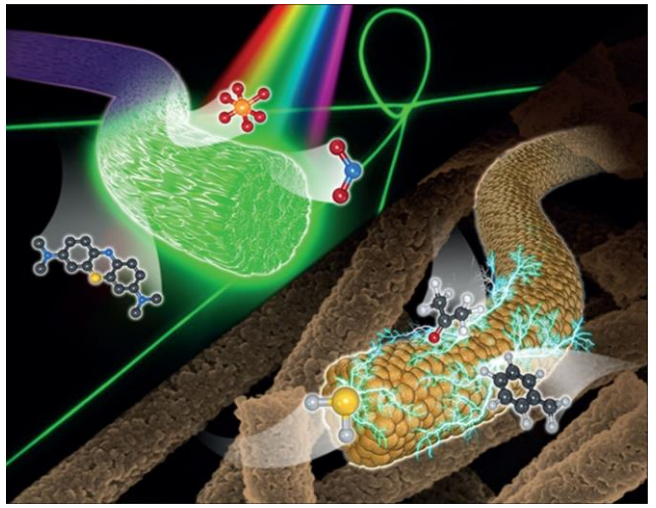

Light-material interactions

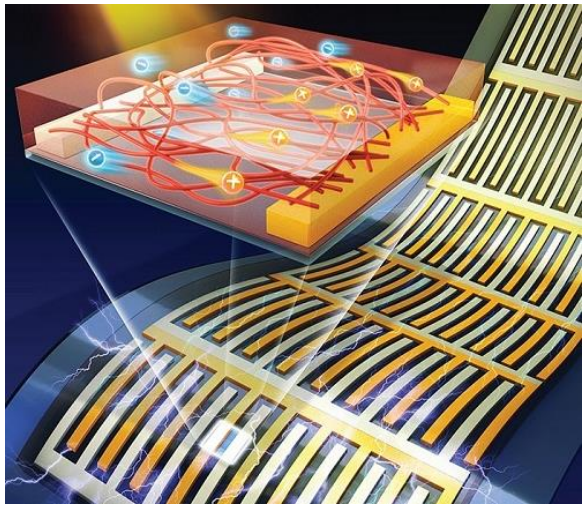

Chemical structure

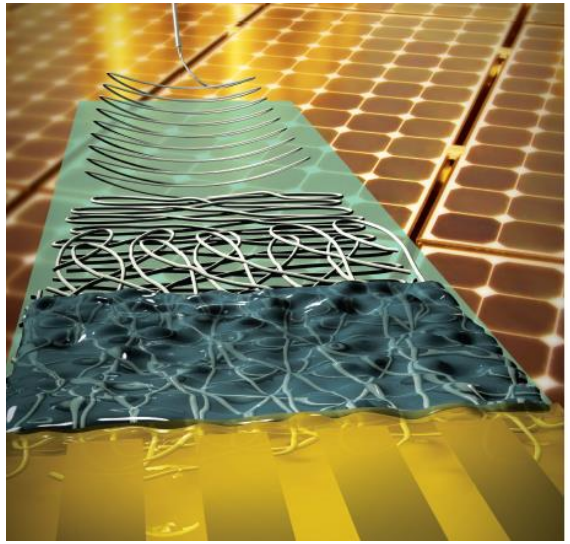

Mechanical properties

Bulk heterojunction (BHJ) solar cells

Mechanism

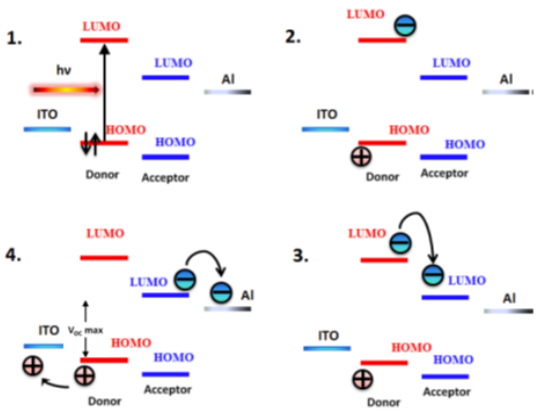

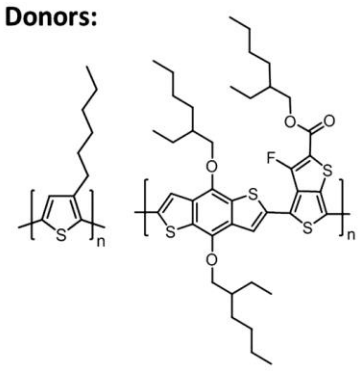

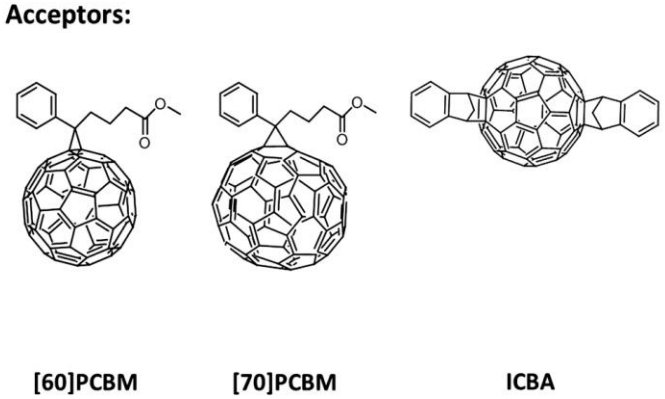

Structure

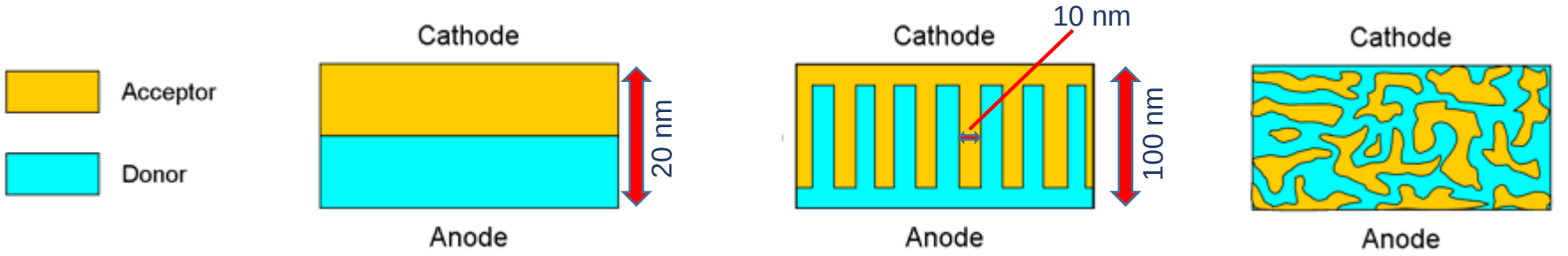

Fabrication

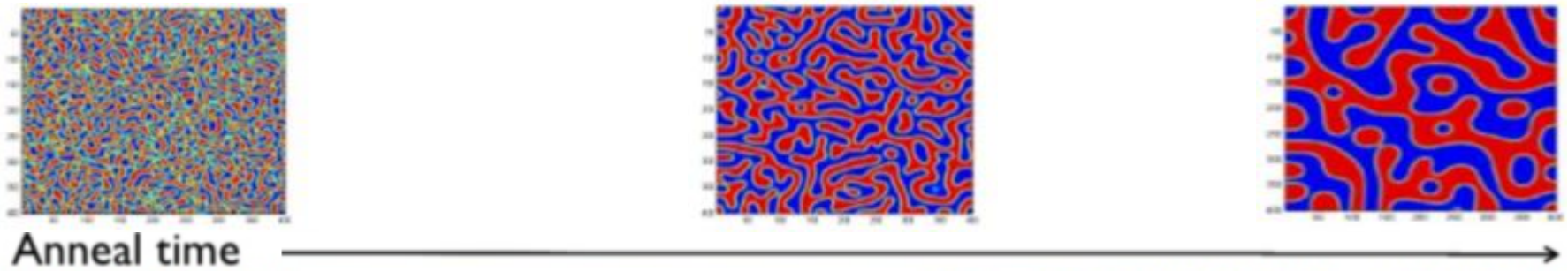

BHJ solar cell limitation

The active material should have a bicontinual and homogeneous nanoscale phase separation, the morphological optimization of this thermodynamically unstable blend is complicated and expensive.

This problem is intrinsic in the concept of BHJ and cannot be completely overcome.

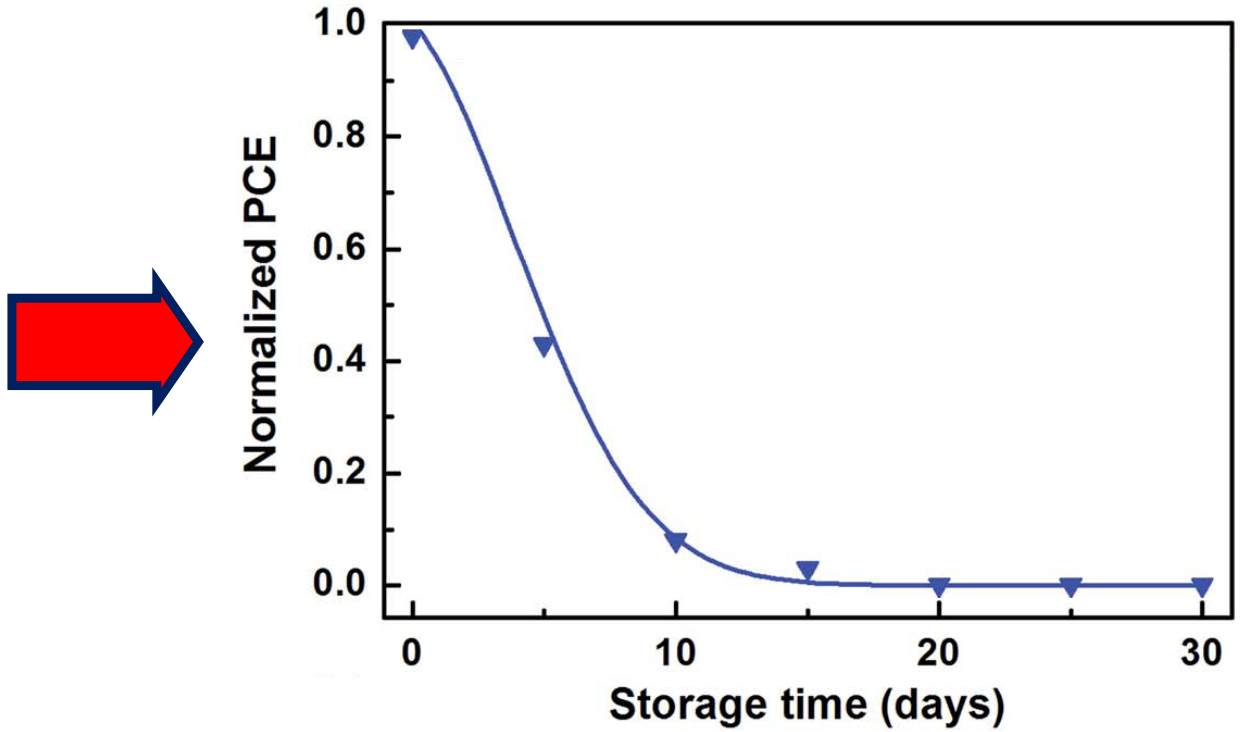

Double-cable polymers

Fullerene-grafted Donor–Acceptor conjugated polymer

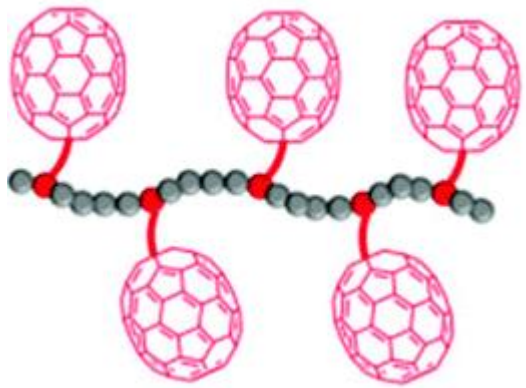

Single-Material Organic Solar Cells (SMOCs)

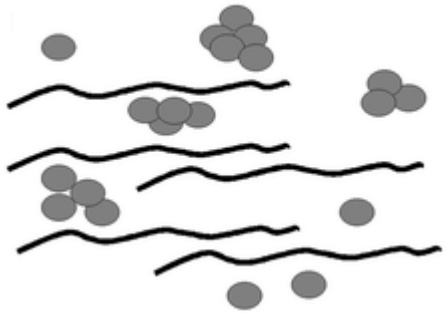

BHJ

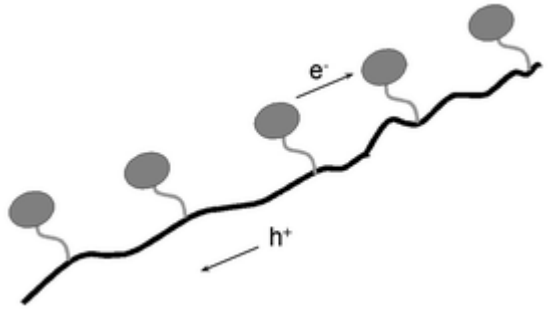

Fullerene-grafted polymer chain

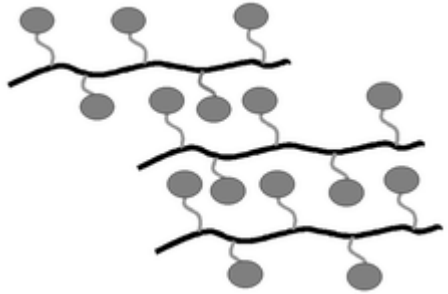

Ordered fullerene-grafted polymer chains

Single-Material Organic Solar Cells (SMOCs)

Disadvantage: low efficiency (PCE: ~3%).

SMOC active layers are considered three-dimensional (3D) structures made of randomly oriented macromolecular units, where charges can move without following the ideal linear path.

Development of efficient transport channels promoting the formation of optimal percolation paths for the charges which is crucial for increasing the SMOC efficiency.

CoP(3DDT)-(C_{60}HT) synthesis

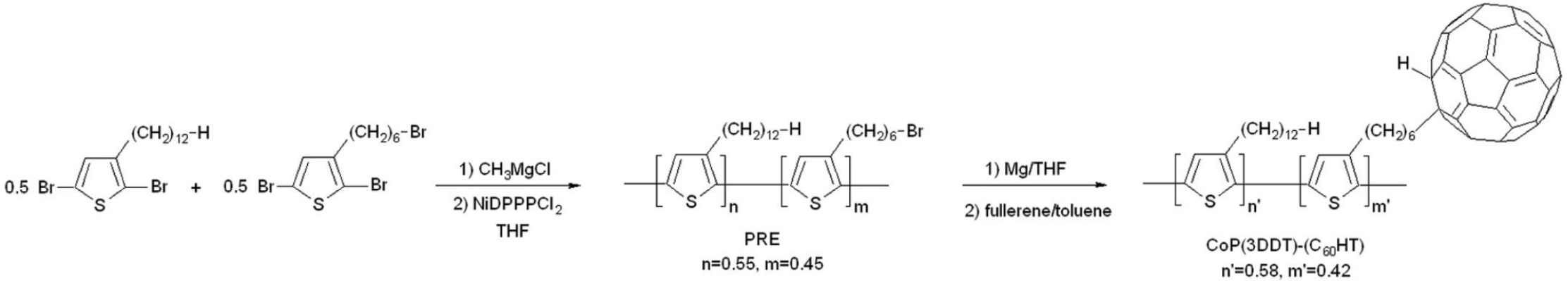

PRE was synthesized through a Grignard metathesis (GRIM) reaction followed by Ni(II)-catalyzed polymerization.

Postpolymerization functionalization (PPF): a bimolecular nucleophilic substitution (S_N2) reaction involving terminal bromine atoms to insert the fullerenic substituent into its side chains.

Synthesis of a new donor−acceptor conjugated copolymer poly[3-dodecylthiophene-co-3-(6-fullerenylhexyl)thiophene] (CoP(3DDT)-(C_{60}HT)), with high:

- fullerene content (maximize the photovoltaic effect)
- regioregularity (well-ordered polymers with close π−π stacking, which is necessary to maximize the charge mobility),
- molecular weight (spinnability)
- solubility (stability)

CoP(3DDT)-(C_{60}HT) characterization

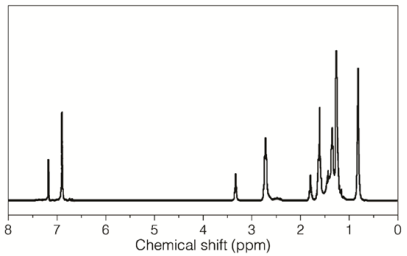

PRE

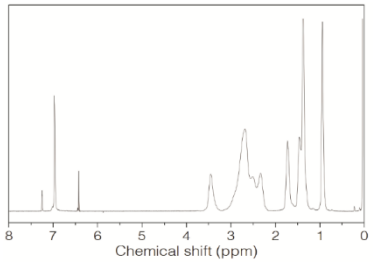

CoP(3DDT)-(C_{60}HT)

Integral ratio of the signal centered at 2.65 ppm (HT dyads) with that at 2.45 ppm (non HT dyads): degree of regioregularity (95% in head-to-tail dyads, HT).

Integral of the methyl group belonging to the alkylic monomer at 0.92 ppm with the integral of the peak at 3.45 ppm, ascribable to the methylene group directly linked to fullerene: copolymer composition (0.58:0.42 molar ratio).

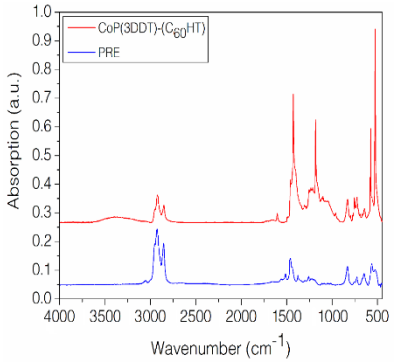

Assignment	PRE (cm^{-1})	CoP(3DDT)-(C_{60}HT) (cm^{-1})
νC-H β thiophene	3049	3049
ν_{as} CH_3	2955	2954
ν_{as} CH_2	2927	2924
ν_{sym} CH_2	2852	2853
ν_{as} C=C thiophene	1510	1545
ν_{as} C=C thiophene	1458	1457
fullerene	-	1429
-CH_3 deformation	1377	1377
fullerene	-	1173
γC-H thioph. 2,3,5-trisubstituted	829	832
νC-Br	561	-
fullerene	-	577
fullerene	-	526

FT-IR spectra of polymers before and after the PFP reaction highlighted the chemical bonding of fullerene.

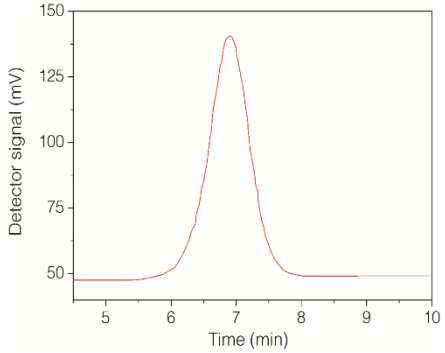

GPC results revealed the high number-average molecular weight (Mn) of CoP(3DDT)-(C_{60}HT), which was 48 000 Da with a narrow polydispersity index (PDI) of around 1.2.

The presence of a dodecyl group in the copolymer structure strongly increased its solubility up to 30 mg/mL in chloroform.

Electrospun CoP(3DDT)-(C_{60}HT) nanofibers

Polymer Solution

CoP(3DDT)-(C_{60}HT) (3.3 wt %) and PEO (0.7 wt %) in chloroform

Electrospinning Parametes

Metal needle with an inner diameter: 0.4 mm
Flow rate: 0.45 mL h^{-1}
Voltage: 8.5 kV
Drum rotation: 2000 rpm
Needle tip-collector distance: 26 cm
Relative humidity: 35%
Temperature: 20 °C

Post-electrospining treatment

the as-spun CoP(3DDT)-(C_{60}HT)/PEO nanofibers were treated by dipping the samples five times in 25 mL of isopropanol for 60 min at 75 °C to remove PEO and obtain pure CoP(3DDT)-(C_{60}HT) nanofibers.

CoP(3DDT)-(C_{60}HT) nanofiber morphology

CoP(3DDT)-(C_{60}HT)/PEO nanofibers

CoP(3DDT)-(C_{60}HT) nanofibers

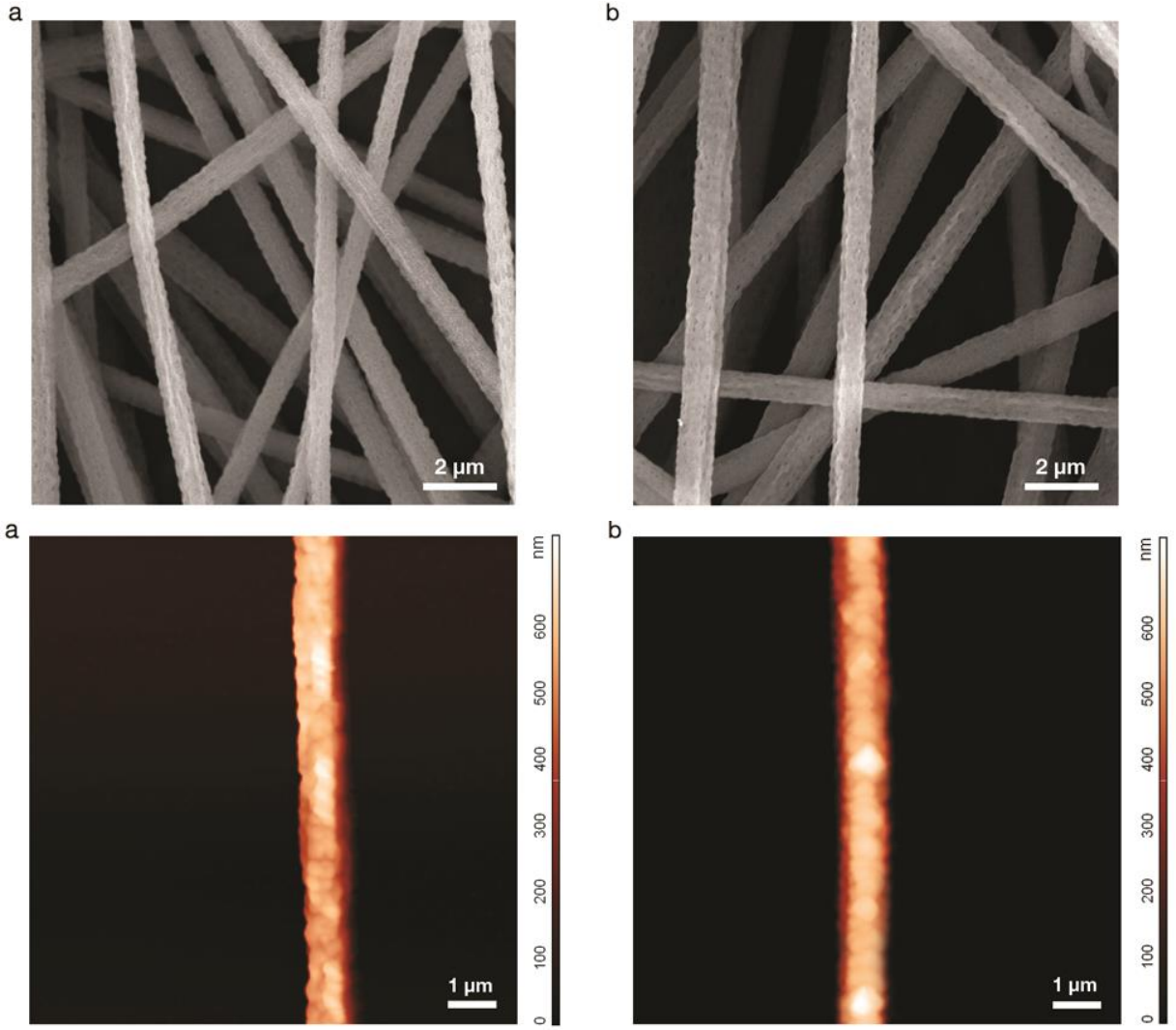

CoP(3DDT)-(C_{60}HT)/PEO: uniform cylindrical fibers with typical textured surfaces (diameters 0.93 ± 0.08 µm).

CoP(3DDT)-(C_{60}HT) with a 0.85 ± 0.12 µm diameter.

The volumetric reduction is consistent with the amount of PEO used to spin nanofibers (17.5%).

PEO removal does not cause any substantial worsening in the material morphology.

The polka-dot surface is due to the removal of PEO. The insulator polymer was located on the external part of the blend nanofibers and tended to form nanoscale domains.

CoP(3DDT)-(C_{60}HT) nanofiber mechanical properties

AFM Nanoindentation

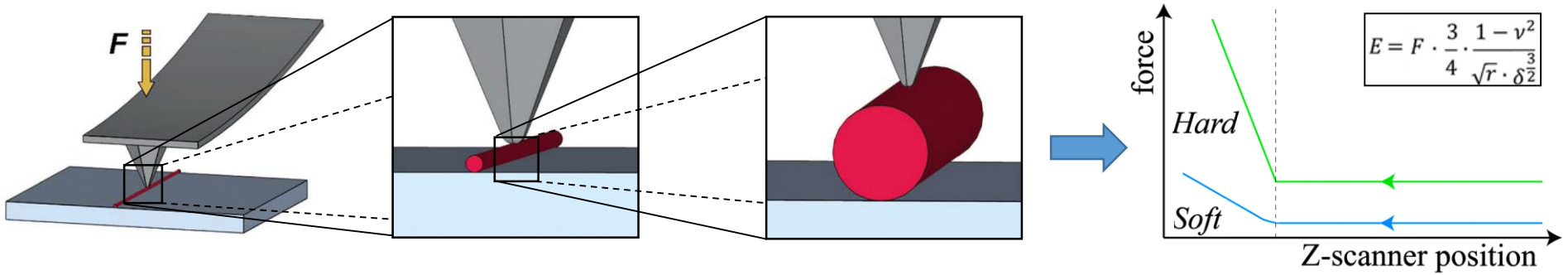

Elastic modulus of CoP(3DDT)-(C_{60}HT) film: 1.59 ± 0.16 GPa

Elastic modulus of CoP(3DDT)-(C_{60}HT) single fibers: 2.52 ± 0.31 GPa

CoP(3DDT)-(C_{60}HT) nanofiber: chemical structure

DSC

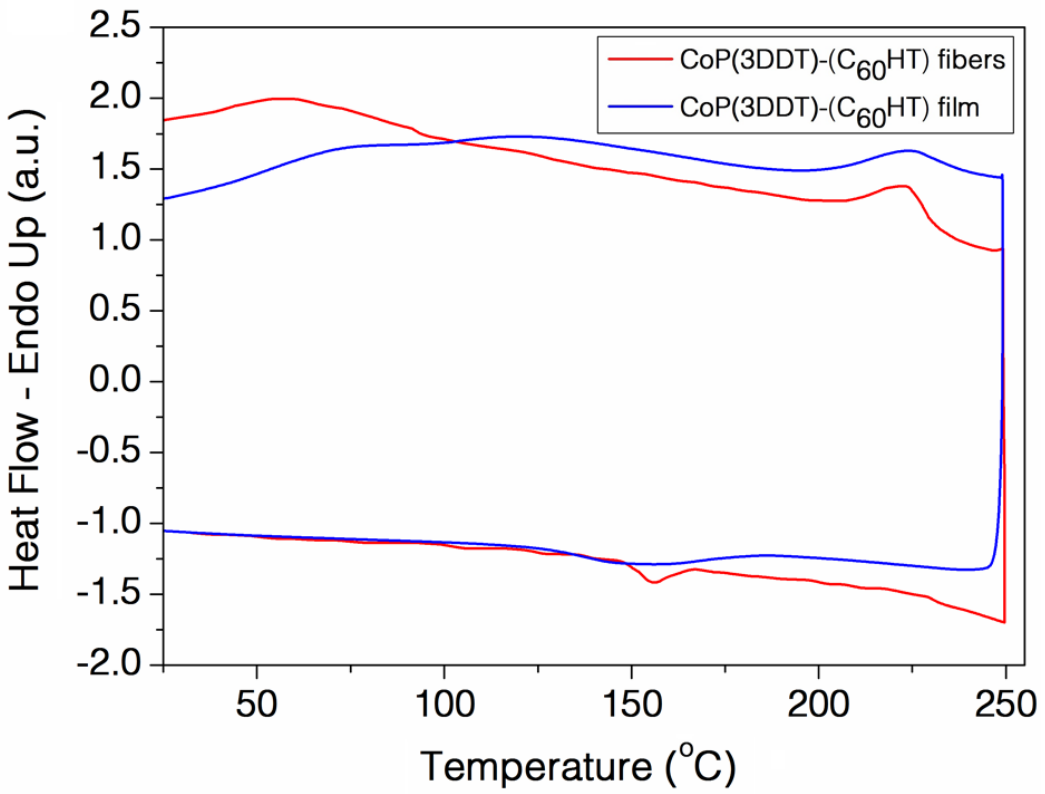

sample	T_g (°C)	T_{m1} (°C)	T_{m2} (°C)	T_c (°C)	ΔH_{m1} (J/g)	ΔH_{m2} (J/g)	ΔH_c (J/g)
CoP(3DDT)-(C_{60}HT) film	52	122	225	148	3.12	5.29	4.62
CoP(3DDT)-(C_{60}HT) fibers	46	120	223	156	0.81	7.40	3.71

CoP(3DDT)-(C_{60}HT) film:

- endothermic flexure at 52 °C (T_g, glass transition temperature).
- endothermic peaks (melting temperatures T_{m1} and T_{m2}) at 122 and 225 °C, melting of crystalline domains determined by the packing of side chains and backbone, respectively.
- exothermic crystallization peak at 148 °C (T_c).

CoP(3DDT)-(C_{60}HT) fibers:

- lower T_{m1} temperature, related to the different spatial disposition of the side chains when electrospun in fibers. The electrospinning fast solvent evaporation that affects the side chain arrangement, as confirmed by a slight decrease in the first melting signal enthalpy (ΔH_{m1}) of the fibers.
- electrospinning has a marked impact on the stretching and alignment of polymer backbone chains, which is highlighted by the increment ΔH_{m2} in the nanofiber sample.

CoP(3DDT)-(C_{60}HT) nanofiber: chemical structure

XRD

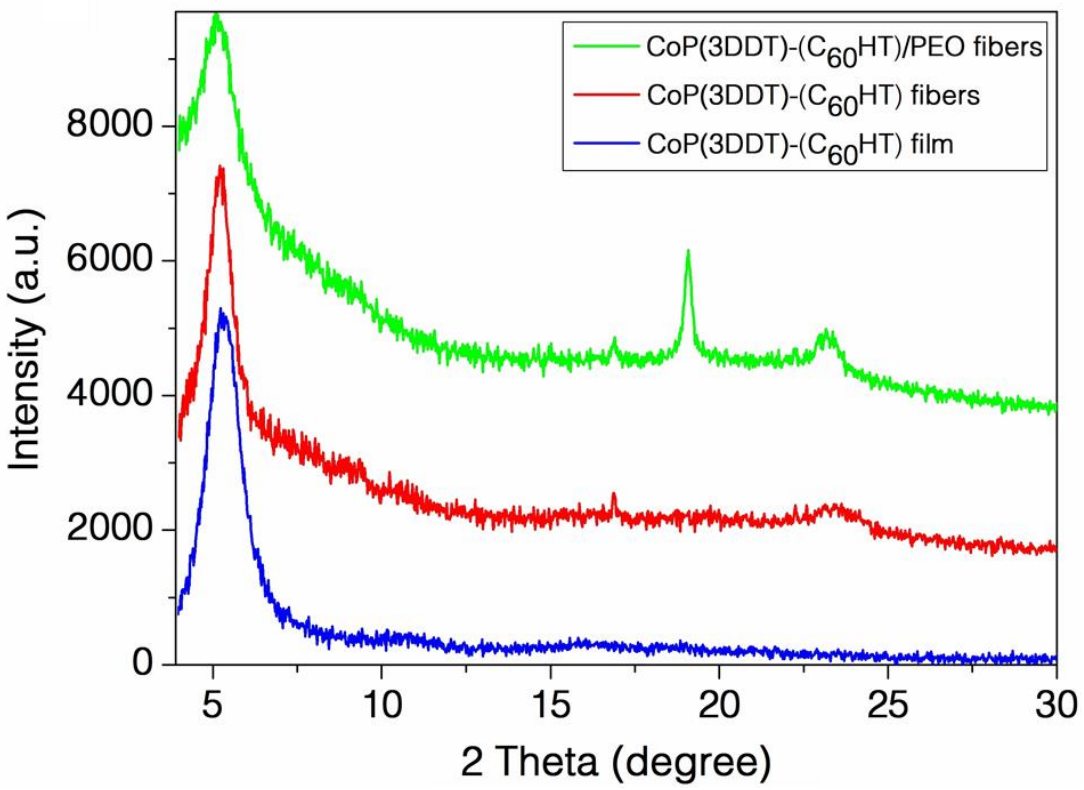

PEO signal (2θ = 19.1°): only in the first sample, confirming the etching process effectiveness.

The (100) reflection due to the CoP(3DDT)-(C_{60}HT) lamellar structures (2θ = 5.1°) became sharper after the postelectrospinning process, thus indicating the development of well-structured copolymer crystallites.

The (010) peak 2θ = 23.5° (π−π interaction) indicates that the indicating that CoP(3DDT)-(C_{60}HT) undergoes backbone chain alignment during the electrospinning process, which promotes the interchain π−π stacking.

Absence of any fullerene aggregation-related peaks. Thanks to the presence of an alkyl spacer between the fullerenes and the backbone.

CoP(3DDT)-(C_{60}HT) nanofiber: chemical structure

UV-Vis

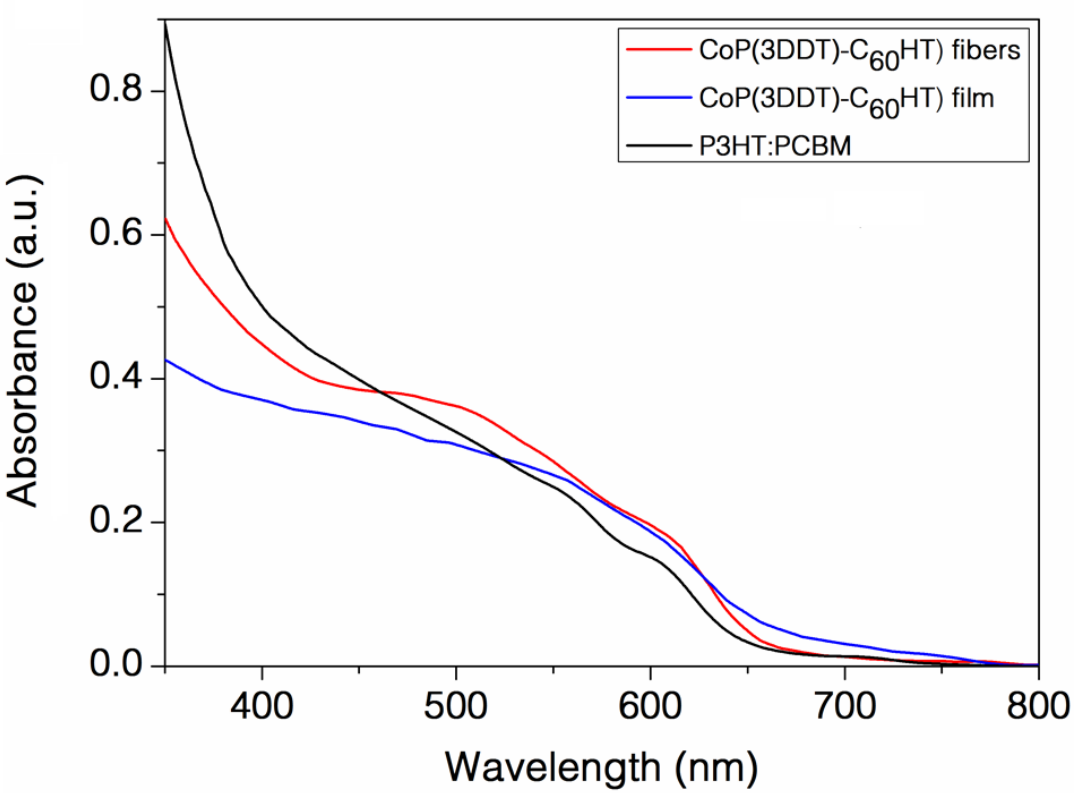

Both CoP(3DDT)-(C_{60}HT) samples show:
(i) an absorbance in the area around 350 nm, which may be ascribed to fullerene derivatives in side chains (more evident in the fiber sample)
(ii) a peak around 500 nm, which may be attributed to the polythiophenic system π−π* transition.

The presence in the electrospun fibers of a further shoulder at around 620 nm, which is usually assigned to noninterdigitating crystalline domains, indicates the formation of π−π stacking between thiophene rings. Furthermore, the absorption shoulder at 620 nm reflects a significant planarization of the polythiophene backbone chains.

The red-shift in nanofiber absorption peaks suggests that polymer chains have a more extended conformation and better delocalized π-conjugation.

Single-Material Organic Solar Cells (SMOCs)

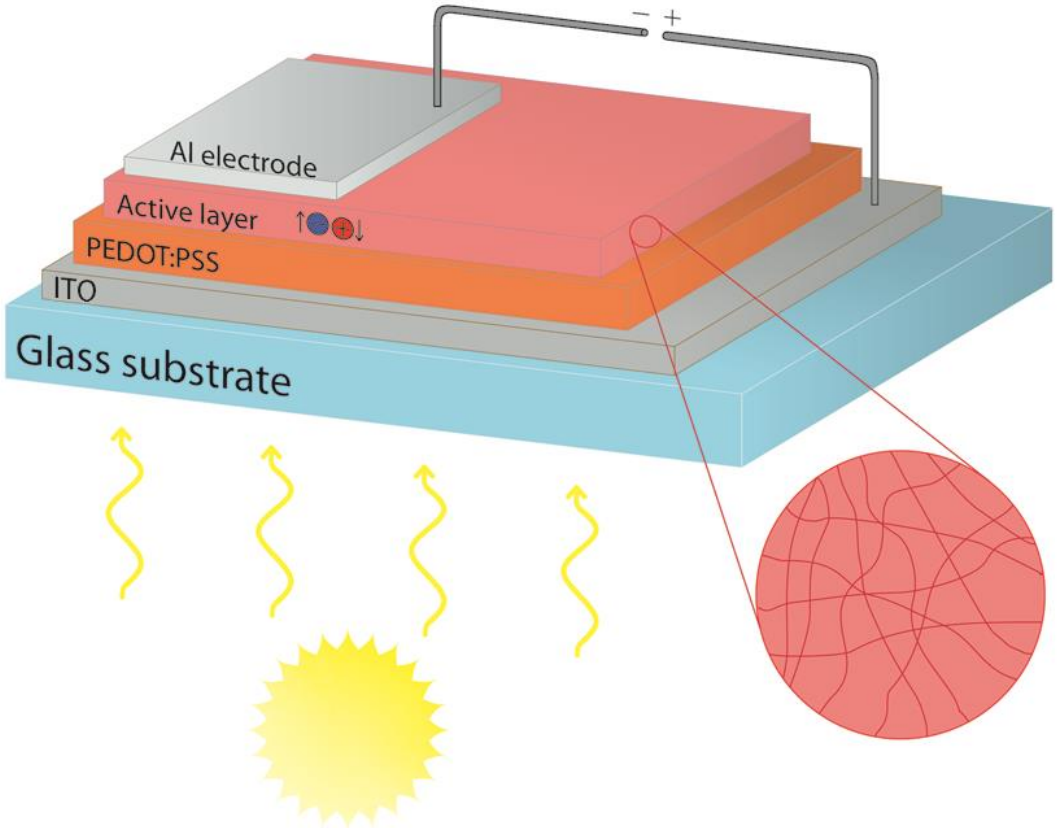

Organic solar cell structure:
Glass slides covered by 80 nm of ITO
PEDOT:PSS layer (120 nm)
Active layers with a 120 nm thickness
Al layer cathode (50 nm)

Active layer composition:
CoP(3DDT)-(C_{60}HT) film
CoP(3DDT)-(C_{60}HT) film (annealed)
CoP(3DDT)-(C_{60}HT) fibers
CoP(3DDT)-(C_{60}HT) fibers (annealed)
BHJ cell (P3HT:PCBM - annealed)

SMOC fabrication

Layer deposition:
Doctor blading

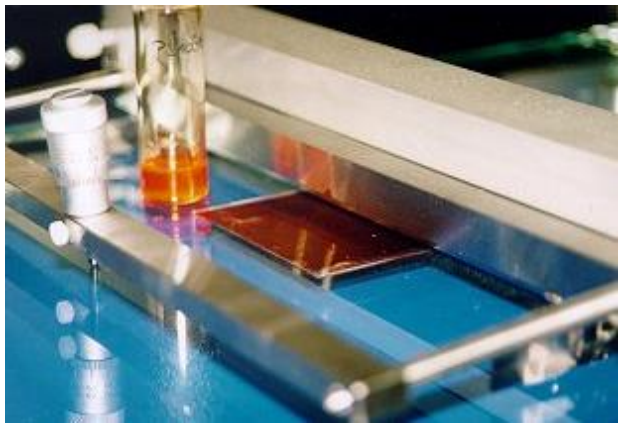

Annealing condition:
heating at 130 °C for 15 min at 10^{-3} mmHg.

Nanofiber incorporation

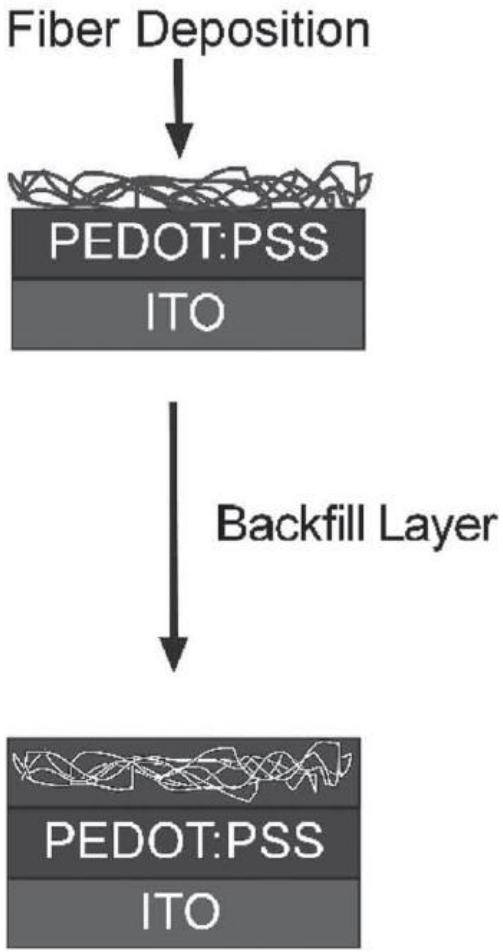

A dispersion of 5 mg of CoP(3DDT)-(C_{60}HT) fibers in 1 mL of cyclohexanone was deposited by doctor blading on the PEDOT:PSS layer.

A backfill layer was deposited on the fiber layer by doctor blading using un unsatured CoP(3DDT)-(C_{60}HT) solution in chlorobenzene.

Fundamental for interconnecting fibers and creating a uniform layer.

The use of an unsaturated solution allows for a further nanofibers diameter reduction while maintaining the structure that serves as a template for the fully solubilized CoP(3DDT)-(C_{60}HT) during the construction of the final layer.

Single-Material Organic Solar Cell: morphology

AFM

Topography | Phase

CoP(3DDT)-(C_{60}HT) film (annealed)

CoP(3DDT)-(C_{60}HT) fiber (annealed)

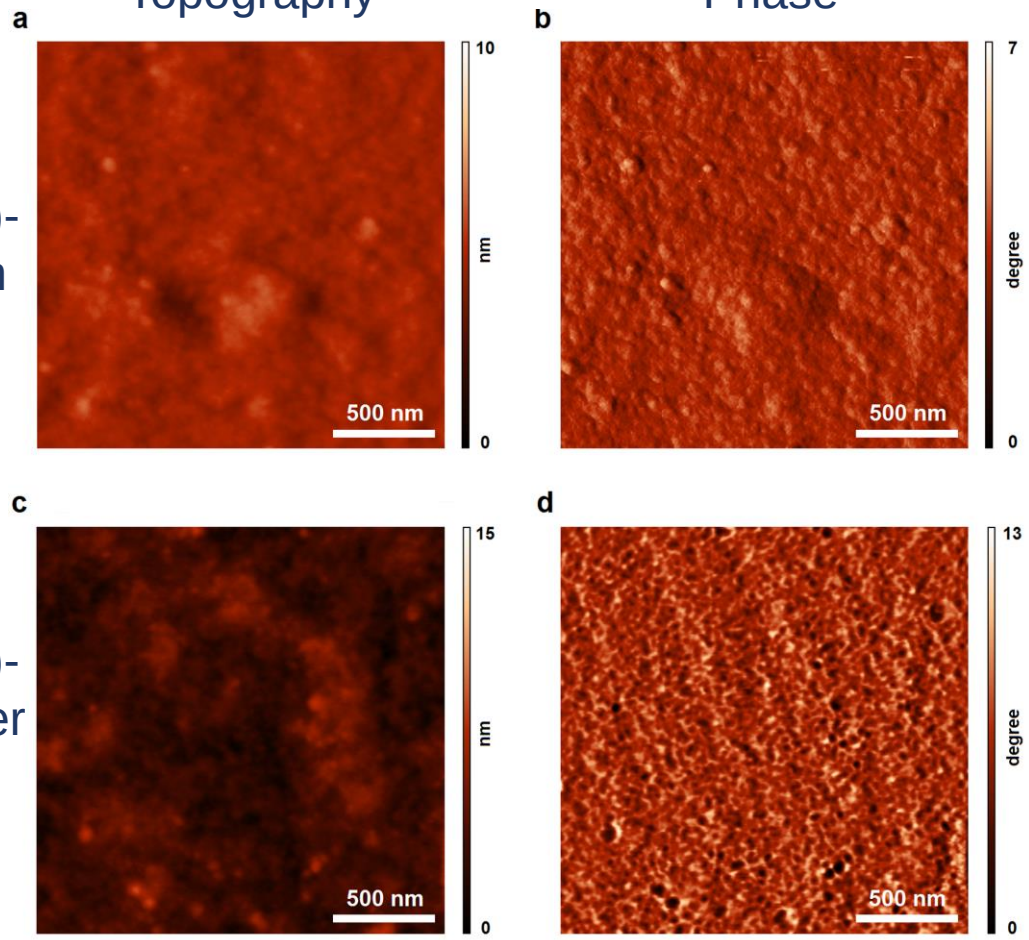

Both height images show flat surfaces with root-mean-square roughness of around 1 nm. The morphology of the film without electrospun nanofibers is more regular than that of fiber-based active materials. The presence of electrospun nanofibers within the cell active layer leads to a slight increment in roughness.

The phase images reveal the absence of large fullerene aggregates in both analyzed materials.

The active layer without fibers shows a featureless phase image, while the presence of a nanopattern is clearly visible in the layer with incorporated electrospun fibers.

The nanopattern formation is often related to the development of higher efficiency devices. This nanopatter has a more spherical morphology than other double-cable active material due to the large number of fullerene groups within the polymer.

Single-Material Organic Solar Cell: photovoltaic performance

External quantum efficiency (EQE) is the ratio of the number of carriers collected by the solar cell to the number of photons of a given energy incident on the solar cell.

$$\mathrm{EQE} = \frac{\text{electrons/sec}}{\text{photons/sec}} = \frac{\text{current}/(\text{charge of one electron})}{(\text{total power of photons})/(\text{energy of one photon})}$$

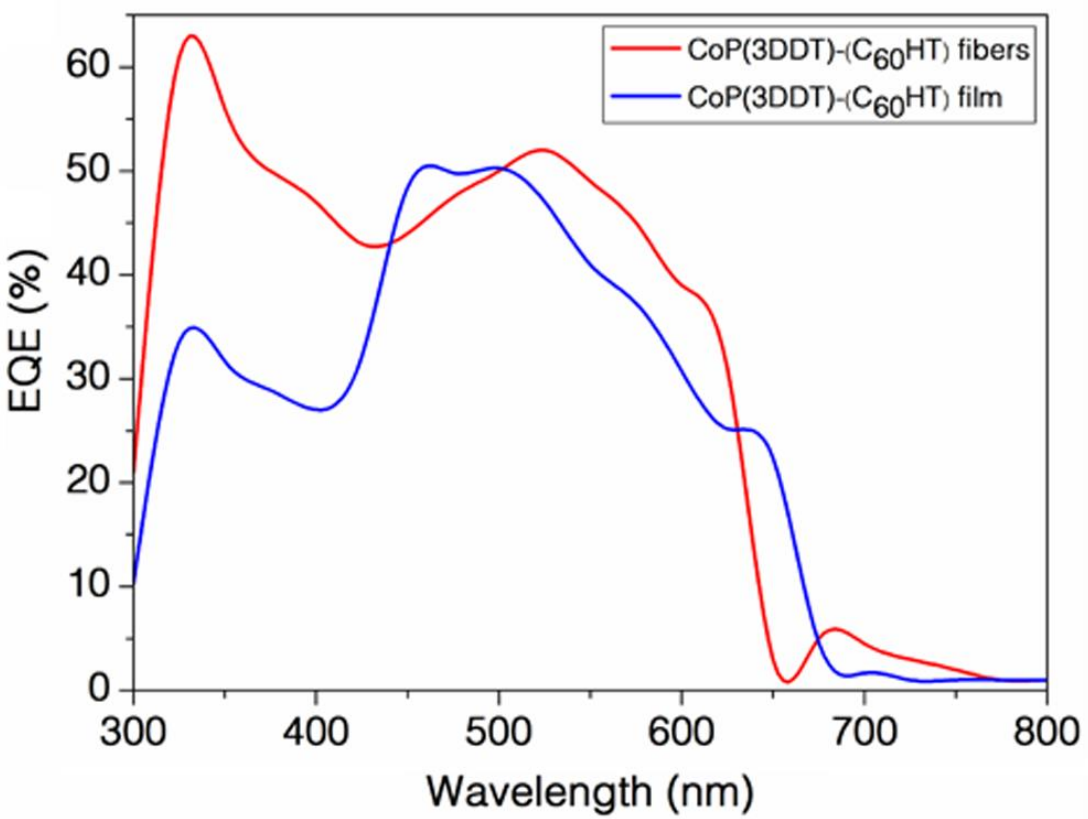

The EQE profiles follow the absorption spectra trend, demonstrating that the harvested photons contribute directly to the photocurrent and confirming the lowering of the recombination side effects.

Maximum EQE in the CoP(3DDT)-(C_{60}HT) fibers reached 61% at around 330 nm, which is remarkably higher than the most intense peak in the SMOCs prepared without fiber (+12.5%). This peak is ascribed to the π−π* transition of chromophoric fullerene derivatives in the side chain. This result highlighted the beneficial effect of the method used on the conformation of both backbone and side polymer chains.

Improvement in quantum efficiency was observed in the 500−625 nm wavelength region, which corresponds to the maximum spectral zone of the solar radiation hitting the Earth's surface.

Single-Material Organic Solar Cell: photovoltaic performance

The power conversion efficiency (PCE) is a photovoltaic cell is the ratio between the maximum electrical power that the array can produce compared to the amount of solar irradiance hitting the cell an it is function of:

$$\eta = \frac{P_{out}}{P_{in}} = \frac{FF \cdot I_{SC} \cdot V_{OC}}{P_{in}}$$

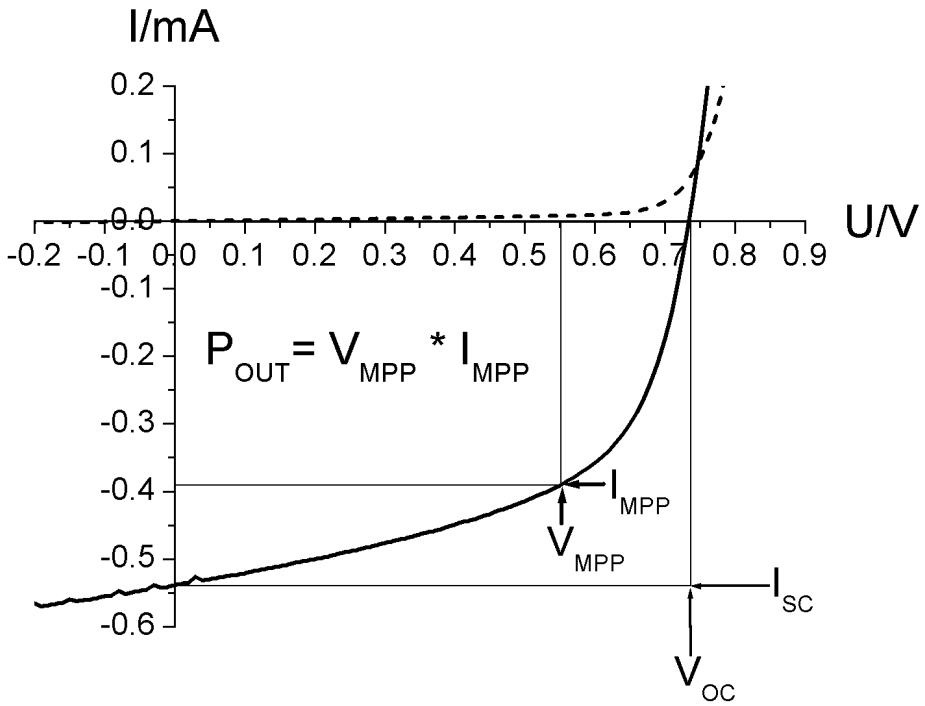

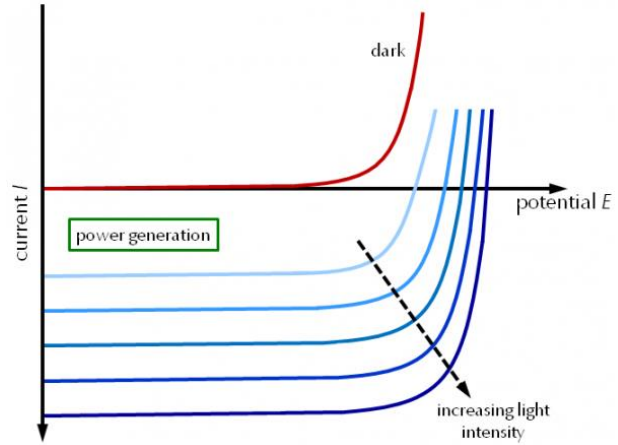

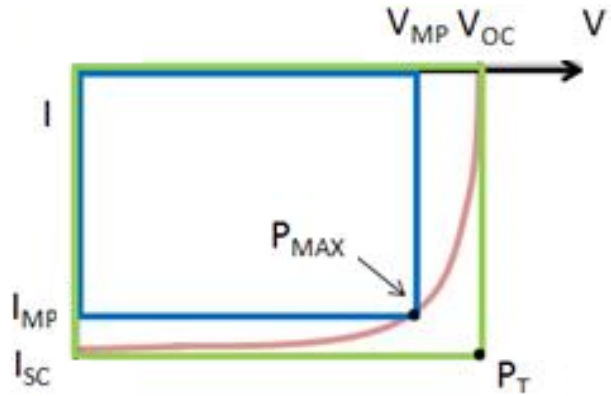

$$FF = \frac{P_{MAX}}{P_T} = \frac{I_{MP} \cdot V_{MP}}{I_{SC} \cdot V_{OC}}$$

Where:

1) V_{OC}: “open circuit voltage“
2) I_{SC}: “short circuit current“
3) FF:“fill factor“
4) P_{out} power delivered
5) P_{in} input power (1000 W/m^2 for an air mass (AM) 1.5 solar simulator)

Single-Material Organic Solar Cell: photovoltaic performance

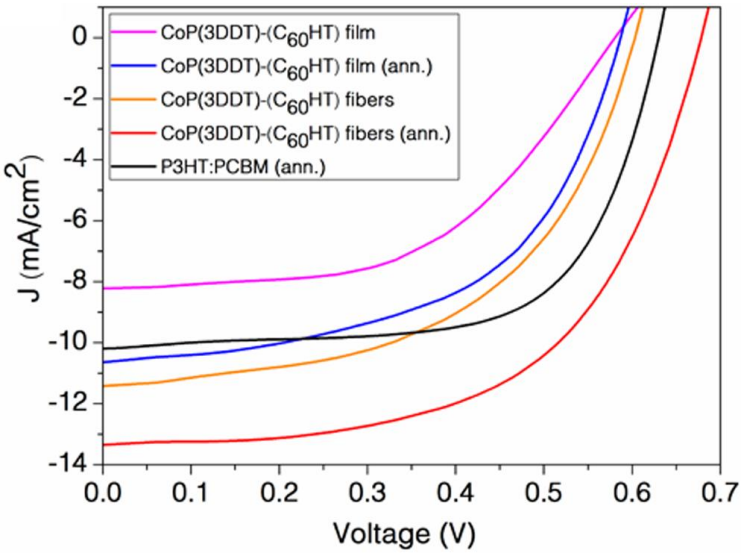

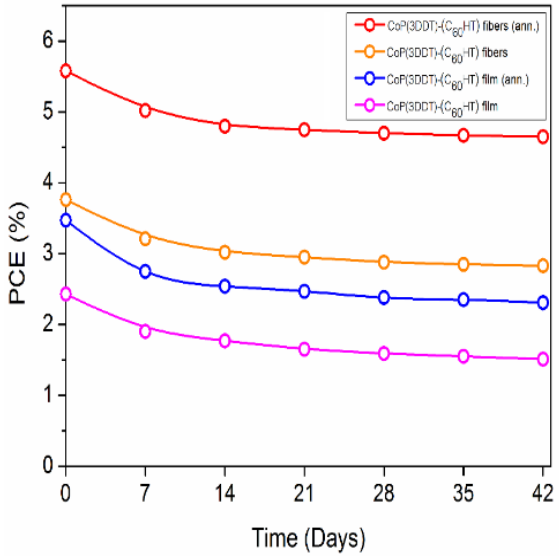

sample	J_{sc} (mA cm^{-2})	V_{oc} (V)	FF (%)	PCE (%)
P3HT:PCBM (annealed)	10.1	0.63	56	3.55
CoP(3DDT)-(C_{60}HT) film	8.2	0.58	51	2.43
CoP(3DDT)-(C_{60}HT) film (annealed)	10.7	0.59	55	3.47
CoP(3DDT)-(C_{60}HT) fibers	11.4	0.60	55	3.76
CoP(3DDT)-(C_{60}HT) fibers (annealed)	13.3	0.68	62	5.58

Solar cells made with a CoP(3DDT)-(C_{60}HT) film and annealed showed a similar PCE to that of the BHJ device (due to the high C_{60} contenent)

The V_{oc} (indicator of the excitons to the carrier collection process – influenced by the charge recombination) values of the BHJ and SMOCs are similar, which proves that it is possible to overcome one of the main double-cable polymer limitations (charge recombination).

Performance improvement achieved by including the nanostructured template into the is attributed to more favorable stacking interactions and side group disposition, permitting a more balanced charge transport.

The fiber-containing cells were more stable than the corresponding ones in film state.
PCE after 42 days:
CoP(3DDT)-(C_{60}HT) fibers (annealed): -16.7%
CoP(3DDT)-(C_{60}HT) film: -37.9%

Single-Material Organic Solar Cell: Conclusions

Novel donor−acceptor polymer (CoP(3DDT)-(C_{60}HT)) with high fullerene group content, high regioregularity, and great solubility may contribute to a greater charge carrier mobility and lower charge recombination.

The presence of the electron-acceptor group chemically linked to the main chain by the alkyl spacer makes it possible to prevent phase-separation phenomena, even at a high fullerene content.

Electrospun CoP(3DDT)-(C_{60}HT) nanofibers were found to have a degree of polymer chain order (interchain π−π stacking and well-structured copolymer system). These features contribute to a more efficient UV−vis radiation absorption, the creation of ideal pathways for charge carriers, and improved mechanical properties.

Thermal annealing strongly contribute to the optimization of the active material structure.

Development of a SMOC with the highest value reported of power conversion efficiency (PCE: 5.58%). +33.2% and +57.2% in terms of efficiency if compared with the best SMOC and a conventional BHJ device, respectively

Future/present objectives: biomedical applications

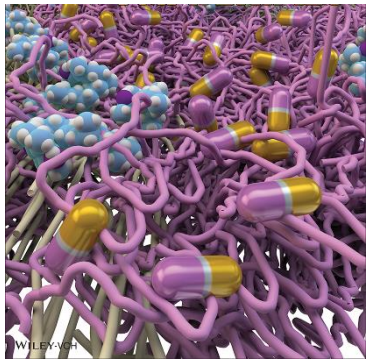

Electrically modulated drug delivery systems

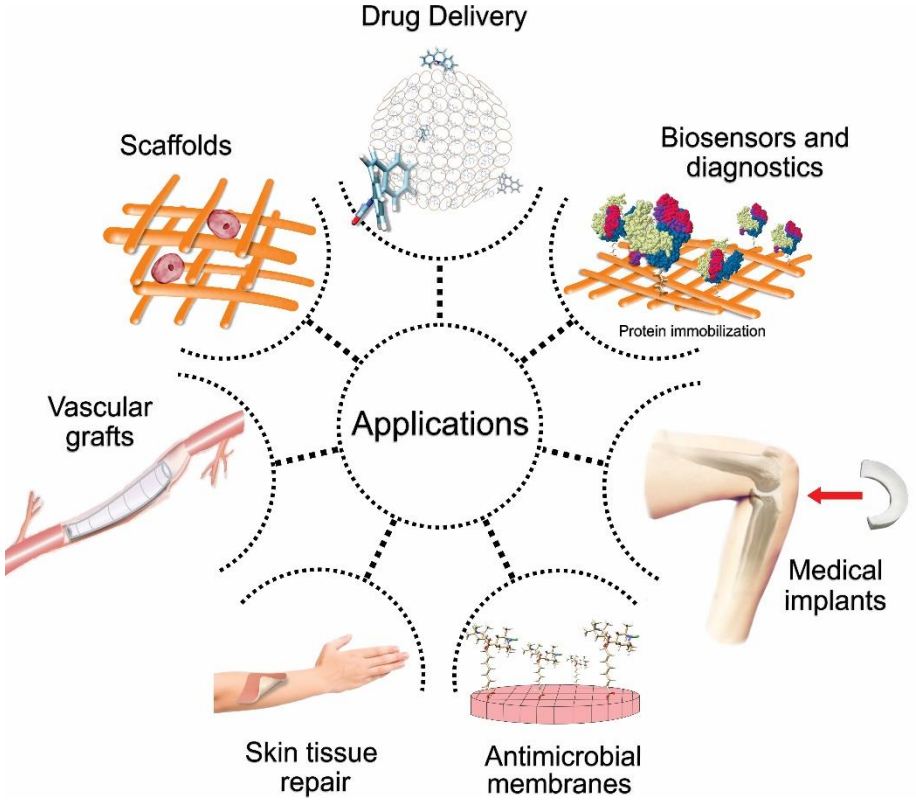

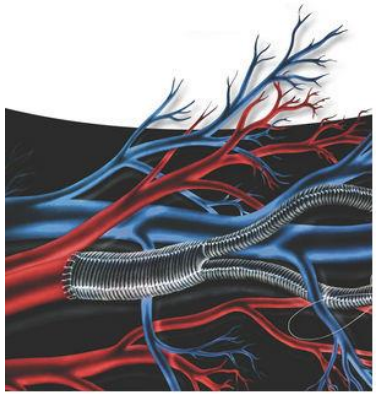

Body–machine interface

Acknowledgements

Institute of Fundamental Technological Research

Department of Biosystems and Soft Matter

Paweł Nakielski

Sylwia Pawłowska

Krzysztof Zembrzycki

Tomasz Kowalewski

Laboratory of Polymers and Biomaterials

Olga Urbanek-Świderska

University of Bologna

Conductive Polymers Research Group

Massimiliano Lanzi